

TwisterForge: controllable and efficient animation of virtual tornadoes

Jiong Chen

Inria / Ecole Polytechnique

James Gain

University of Cape Town

Jean-Marc Chomaz

Ecole Polytechnique

Marie-Paule Cani

Ecole Polytechnique

**MIG
2024**
Arlington

Inria



TORNADO OUTBREAKS

The frequency of U.S. outbreaks with many tornadoes is increasing and it is increasing faster for more extreme outbreaks.

TORNADOES

More tornadoes in the most extreme U.S. tornado outbreaks

Michael K. Tippett,^{1,2*} Chiara Lepore,³ Joel E. Cohen^{4,5,6}

Tornadoes and severe thunderstorms kill people and damage property every year. Estimated U.S. insured losses due to severe thunderstorms in the first half of 2016 were \$8.5 billion (US). The largest U.S. effects of tornadoes result from tornado outbreaks, which are sequences of tornadoes that occur in close succession. Here, using extreme value analysis, we find that the frequency of U.S. outbreaks with many tornadoes is increasing and that it is increasing faster for more extreme outbreaks. We model this behavior by extreme value distributions with parameters that are linear functions of time or of some indicators of multidecadal climatic variability. Extreme meteorological environments associated with severe thunderstorms show consistent upward trends, but the trends do not resemble those currently expected to result from global warming.

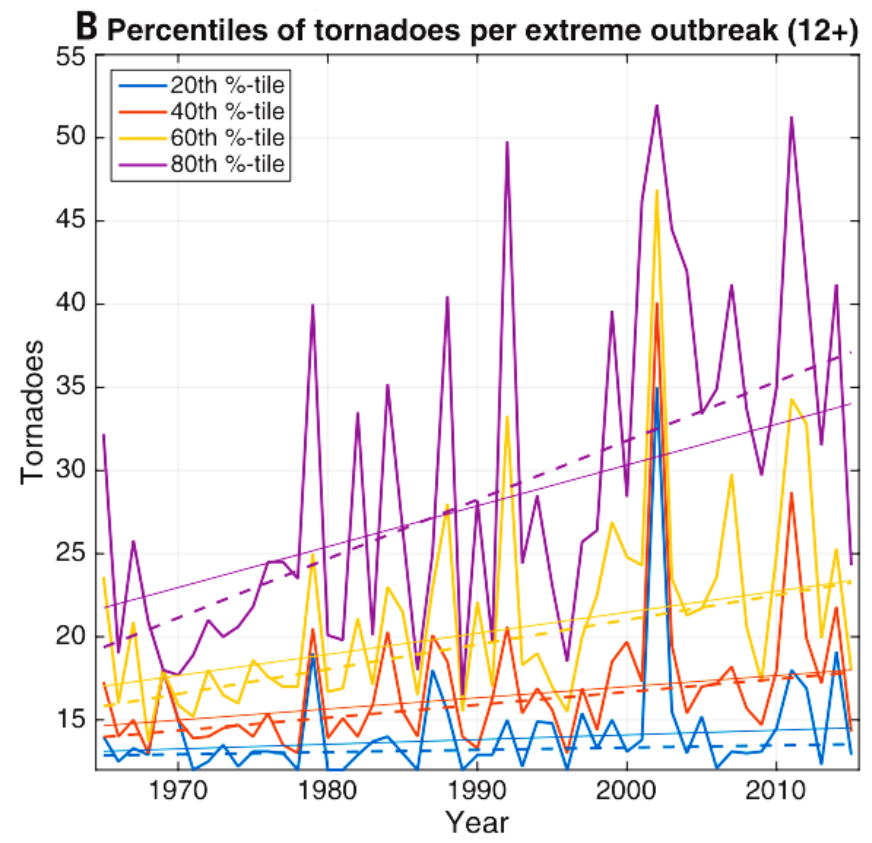
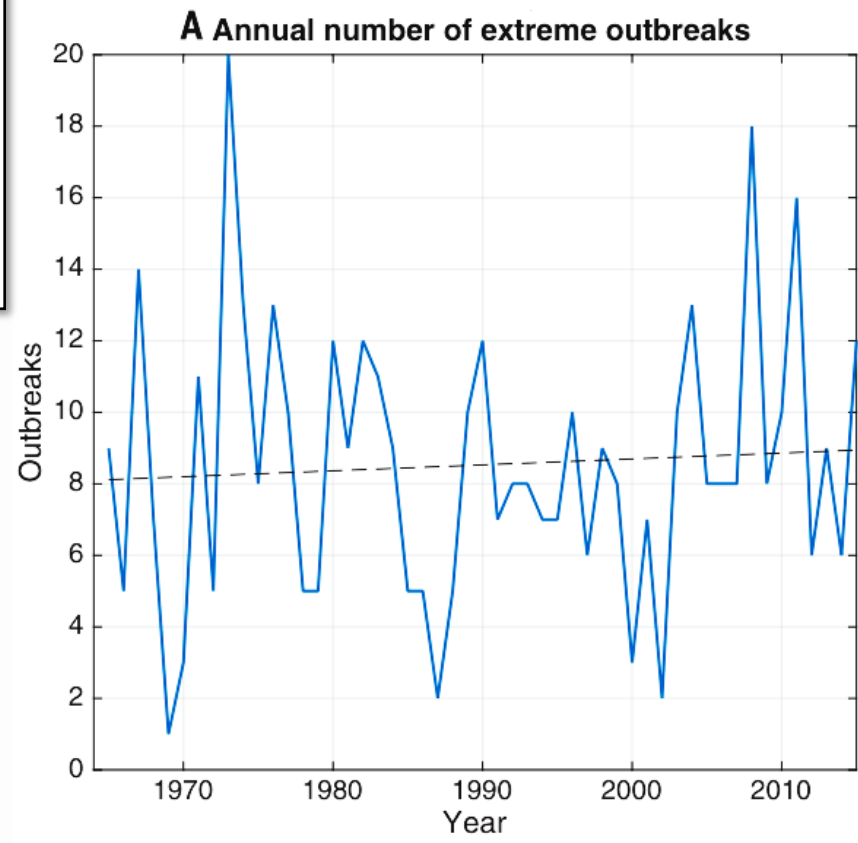
In the United States, tornado outbreaks have substantial effects on human lives and property. Tornado outbreaks are sequences of six or more tornadoes that are rated F1 and greater on the Fujita scale or rated EF1 and greater on the Enhanced Fujita scale and that occur in close succession (1, 2). About 79% of tornado fatalities during the period 1972 to 2010 occurred in outbreaks (3), and 35 people died in U.S. tornado outbreaks in 2015. No significant trends have been found in either the annual number of reliably reported tornadoes (3) or of outbreaks (7). However, recent studies indicate increased variability in large normalized economic and insured losses from U.S. thunderstorms (4), increases in the annual number of

days on which many tornadoes occur (3, 5), and increases in the annual mean and variance of the number of tornadoes per outbreak (6). Here, using extreme value analysis, we find that the frequency of U.S. outbreaks with many tornadoes is increasing and that it is increasing faster for more extreme outbreaks. We model this behavior by extreme value distributions with parameters that are linear functions of time or of some indicators of multidecadal climatic variability. Extreme meteorological environments associated with severe thunderstorms show consistent upward trends, but the trends do not resemble those currently expected to result from global warming.

Linear trends in the percentiles of the number of tornadoes per outbreak (Fig. 1A) are positive, statistically significant, and increase exponentially faster with percentile probability (Fig. 1B). This behavior is consistent with the positive trends in

¹Department of Applied Physics and Applied Mathematics, Columbia University, New York, NY, USA; ²Center of Excellence for Climate Change Research, Department of Meteorology, King Abdulaziz University, Jeddah, Saudi Arabia; ³Samuel Dineen Earth Observatory, Columbia University, Palisades, NY 10964, USA; ⁴Laboratory of Populations, Rockefeller University, New York, NY 10065, USA; ⁵The Earth Institute and Department of Statistics, Columbia University, New York, NY 10027, USA; ⁶Department of Statistics, University of Chicago, Chicago, IL 60637, USA. *Corresponding author. Email: mt14@columbia.edu

[Tippett et al. 2016], Science



TORNADO ANIMATION FOR ENTERTAINMENT



Movies



Video games



PHYSICALLY BASED NUMERICAL SIMULATION

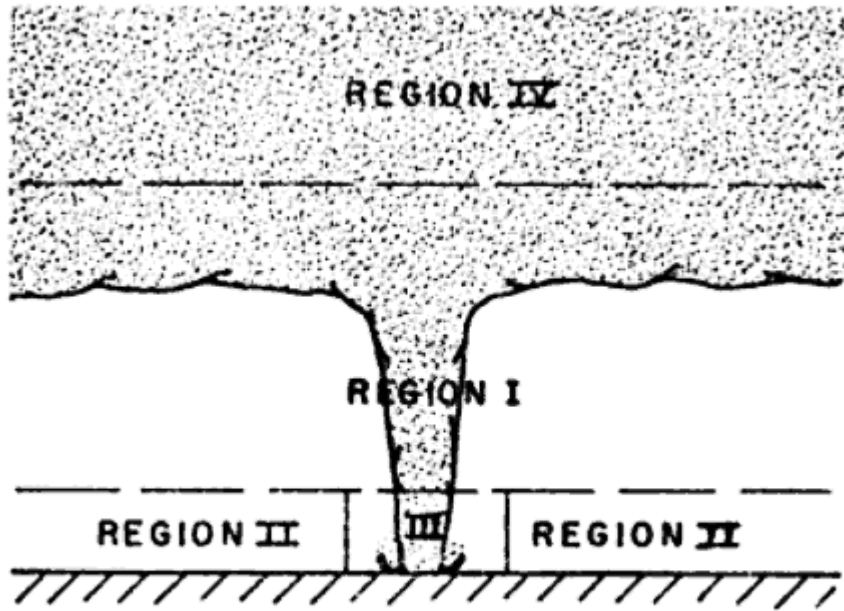
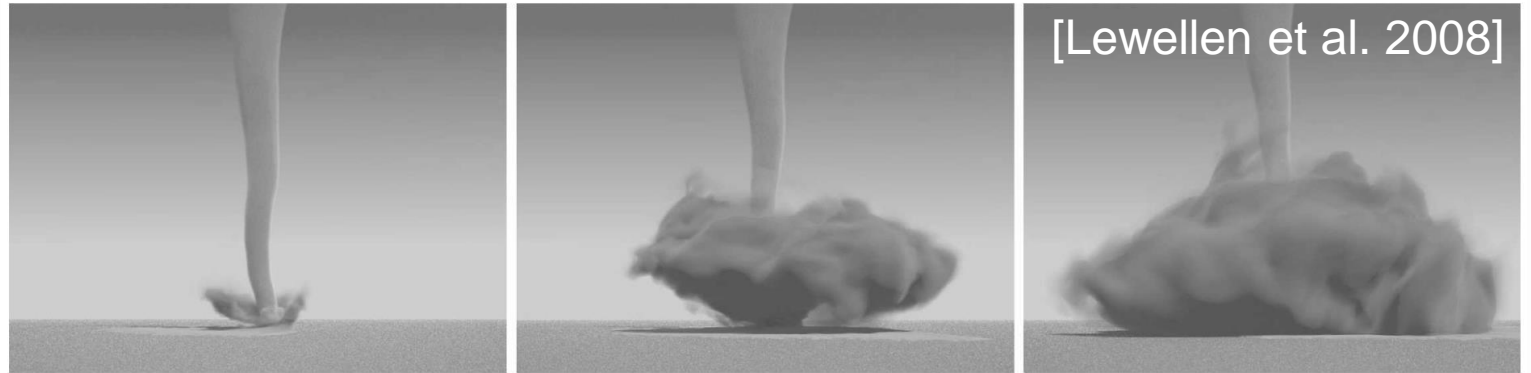


Fig. 1. Sketch showing the division of the tornado into four separate regions.

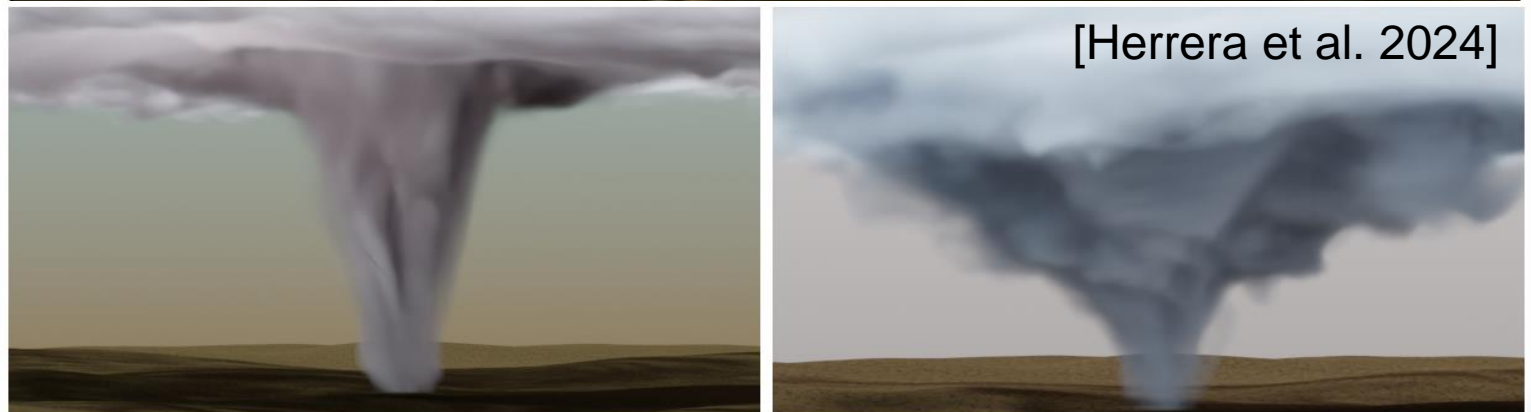
[Lewellen 1976]



[Lewellen et al. 2008]



[Liu et al. 2008]



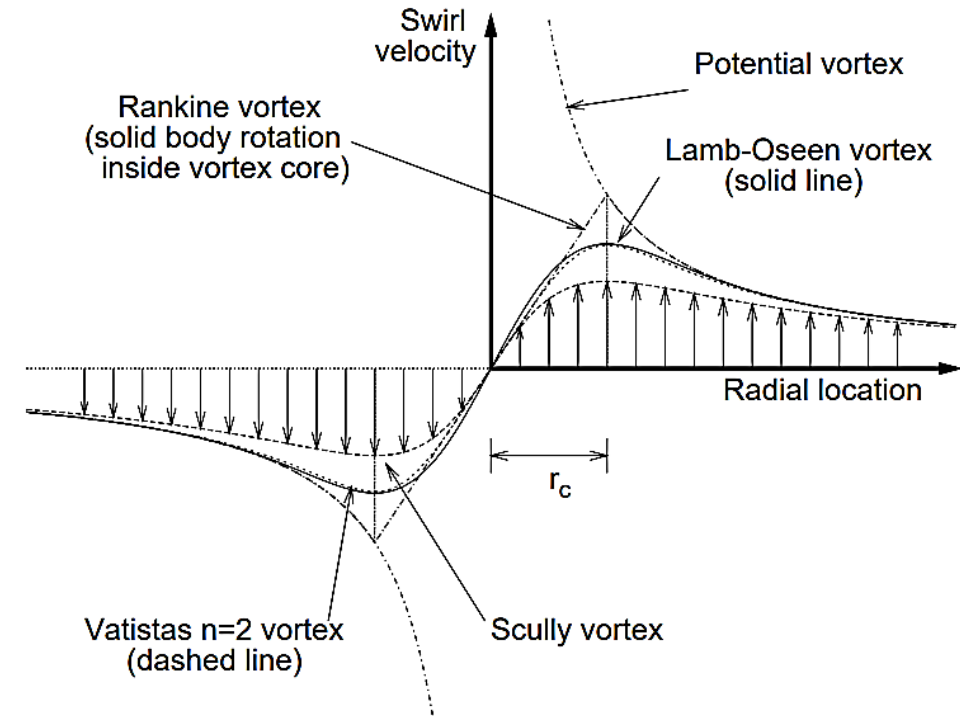
[Herrera et al. 2024]

ANALYTICAL VORTEX SOLUTIONS

- Simplify the 3D NS equation
 - Assuming helical symmetry of the flow

Axisymmetric steady flow

$$\left\{ \begin{array}{l} v_r \frac{\partial v_r}{\partial r} + v_z \frac{\partial v_r}{\partial z} - \frac{v_\theta^2}{r} = \\ \quad - \frac{1}{\rho} \frac{\partial p}{\partial r} + \mu \left(\frac{1}{r} \frac{\partial}{\partial r} \left(r \frac{\partial v_r}{\partial r} \right) + \frac{\partial^2 v_r}{\partial z^2} - \frac{v_r}{r^2} \right), \\ v_r \frac{\partial v_\theta}{\partial r} + v_z \frac{\partial v_\theta}{\partial z} + \frac{v_\theta v_r}{r} = \mu \left(\frac{1}{r} \frac{\partial}{\partial r} \left(r \frac{\partial v_\theta}{\partial r} \right) - \frac{v_\theta}{r^2} \right), \\ v_r \frac{\partial v_z}{\partial r} + v_z \frac{\partial v_z}{\partial z} = - \frac{1}{\rho} \frac{\partial p}{\partial z} + \mu \left(\frac{1}{r} \frac{\partial}{\partial r} \left(r \frac{\partial v_z}{\partial r} \right) \right), \end{array} \right.$$

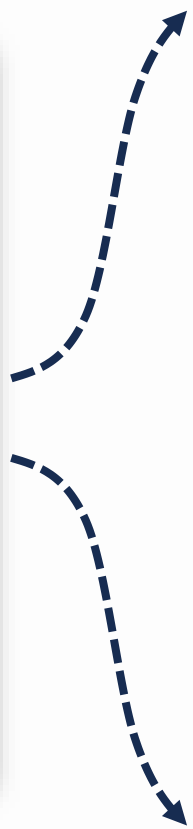


OUR APPROACH

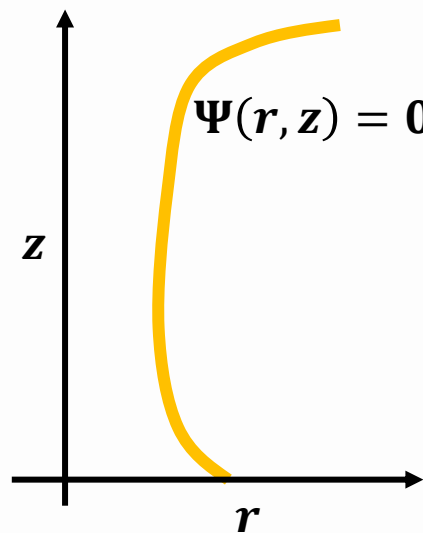
A core-and-funnel model



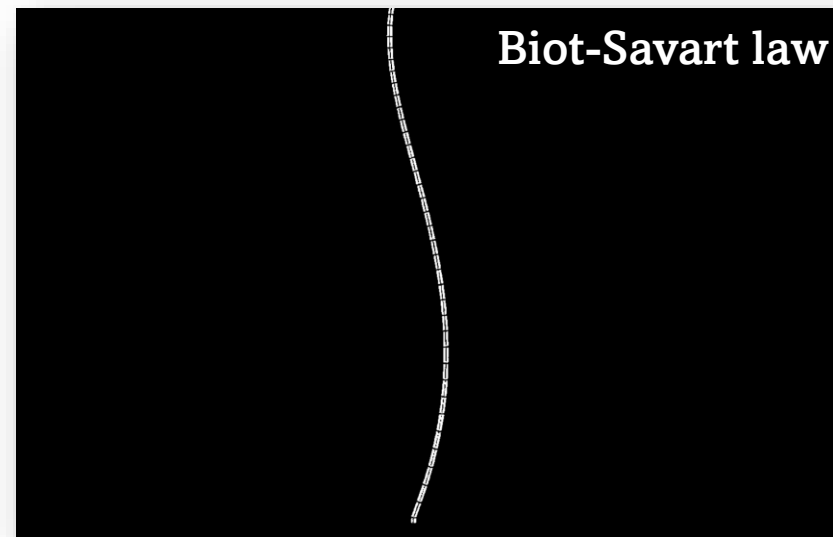
Vortex filament



Stokes stream function



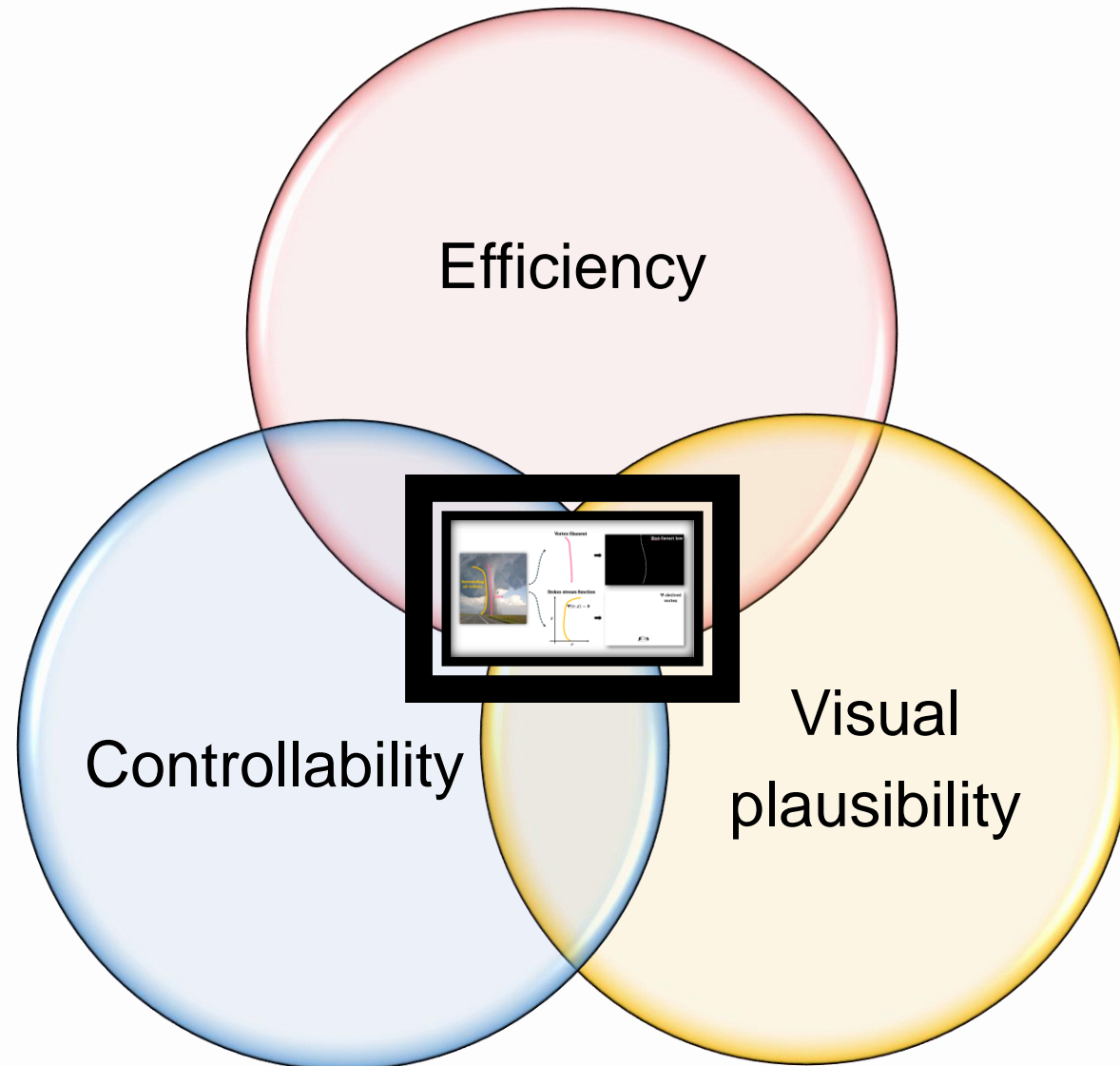
Biot-Savart law



Ψ -derived vortex



GOAL

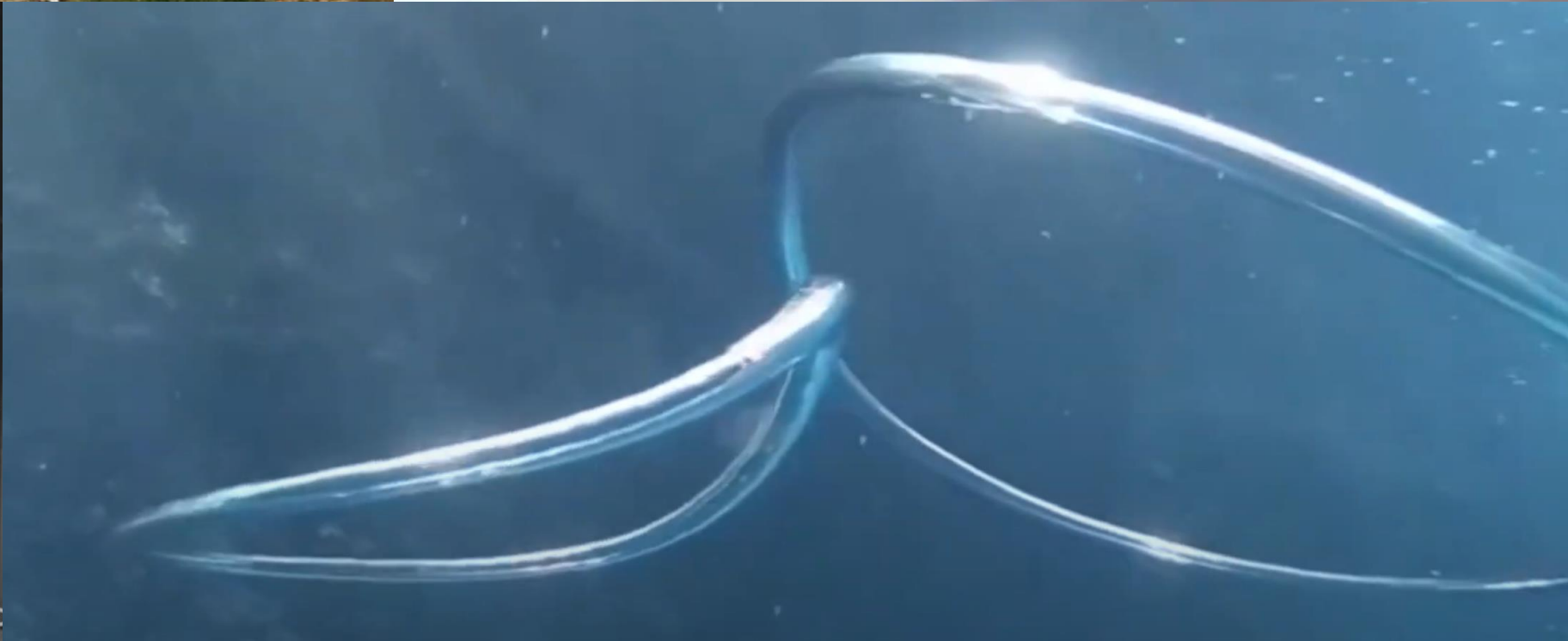


Tornado Core



EXAMPLES OF VORTEX FILAMENT

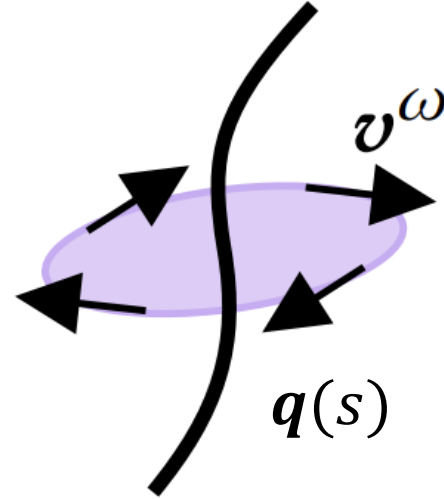
A slender, tube-like region of swirling fluid with concentrated vorticity (rotation).



VORTEX FILAMENT KINEMATICS

- Velocity around a vortex filament, i.e., Biot-Savart law

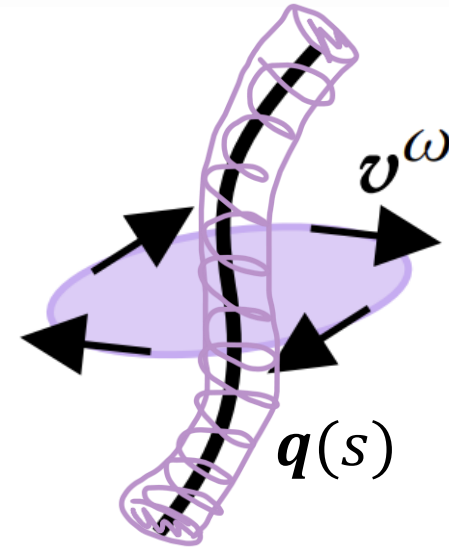
$$\mathbf{v}^\omega(\mathbf{p}) = -\frac{\Gamma}{4\pi} \int_0^L \frac{(\mathbf{p} - \mathbf{q}(s)) \times \partial_s \mathbf{q}}{(\|\mathbf{p} - \mathbf{q}(s)\|^2 + \mu^2)^{\frac{3}{2}}} ds,$$



VORTEX FILAMENT KINEMATICS

- Velocity around a vortex filament, i.e., Biot-Savart law

$$\mathbf{v}^\omega(\mathbf{p}) = -\frac{\Gamma}{4\pi} \int_0^L \frac{(\mathbf{p} - \mathbf{q}(s)) \times \partial_s \mathbf{q}}{(\|\mathbf{p} - \mathbf{q}(s)\|^2 + \mu^2)^{\frac{3}{2}}} ds,$$



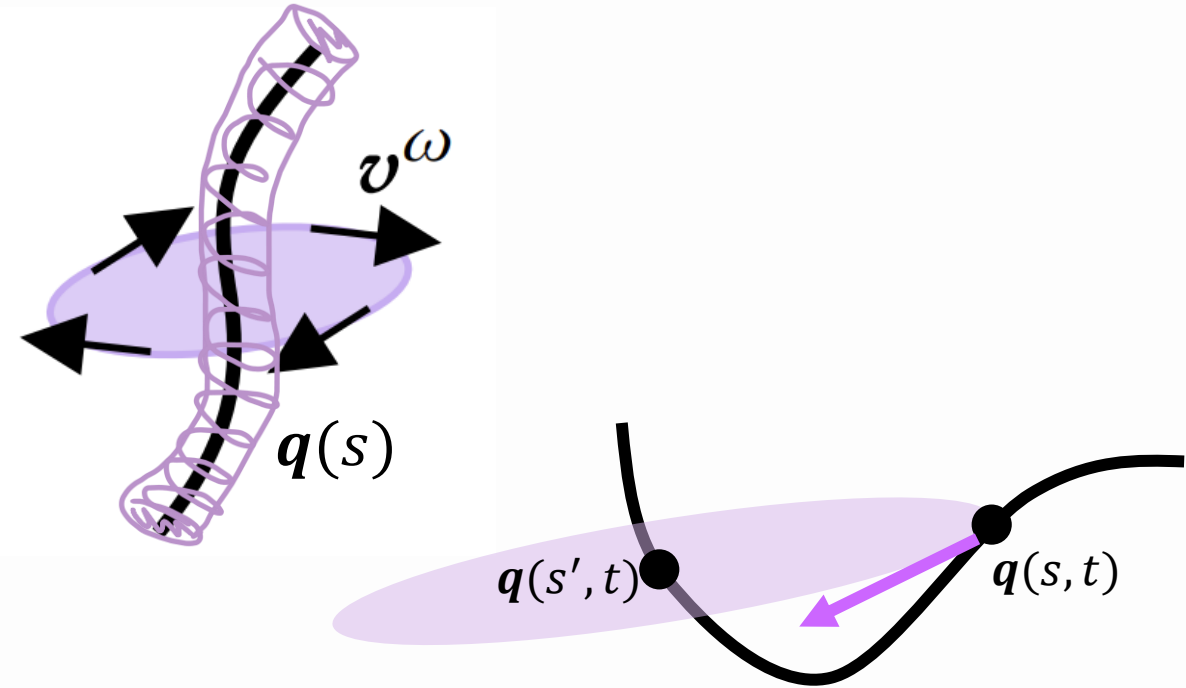
VORTEX FILAMENT KINEMATICS

- Velocity around a vortex filament, i.e., Biot-Savart law

$$\mathbf{v}^\omega(\mathbf{p}) = -\frac{\Gamma}{4\pi} \int_0^L \frac{(\mathbf{p} - \mathbf{q}(s)) \times \partial_s \mathbf{q}}{(\|\mathbf{p} - \mathbf{q}(s)\|^2 + \mu^2)^{\frac{3}{2}}} ds,$$

- Core kinematics by self-advection

$$\frac{\partial \mathbf{q}}{\partial t} = \mathbf{v}^\omega(\mathbf{q}) = -\frac{\Gamma}{4\pi} \int_0^L \frac{[\mathbf{q}(s, t) - \mathbf{q}(s', t)] \times \partial_{s'} \mathbf{q}}{(\|\mathbf{q}(s) - \mathbf{q}(s')\|^2 + \mu^2)^{\frac{3}{2}}} ds'.$$



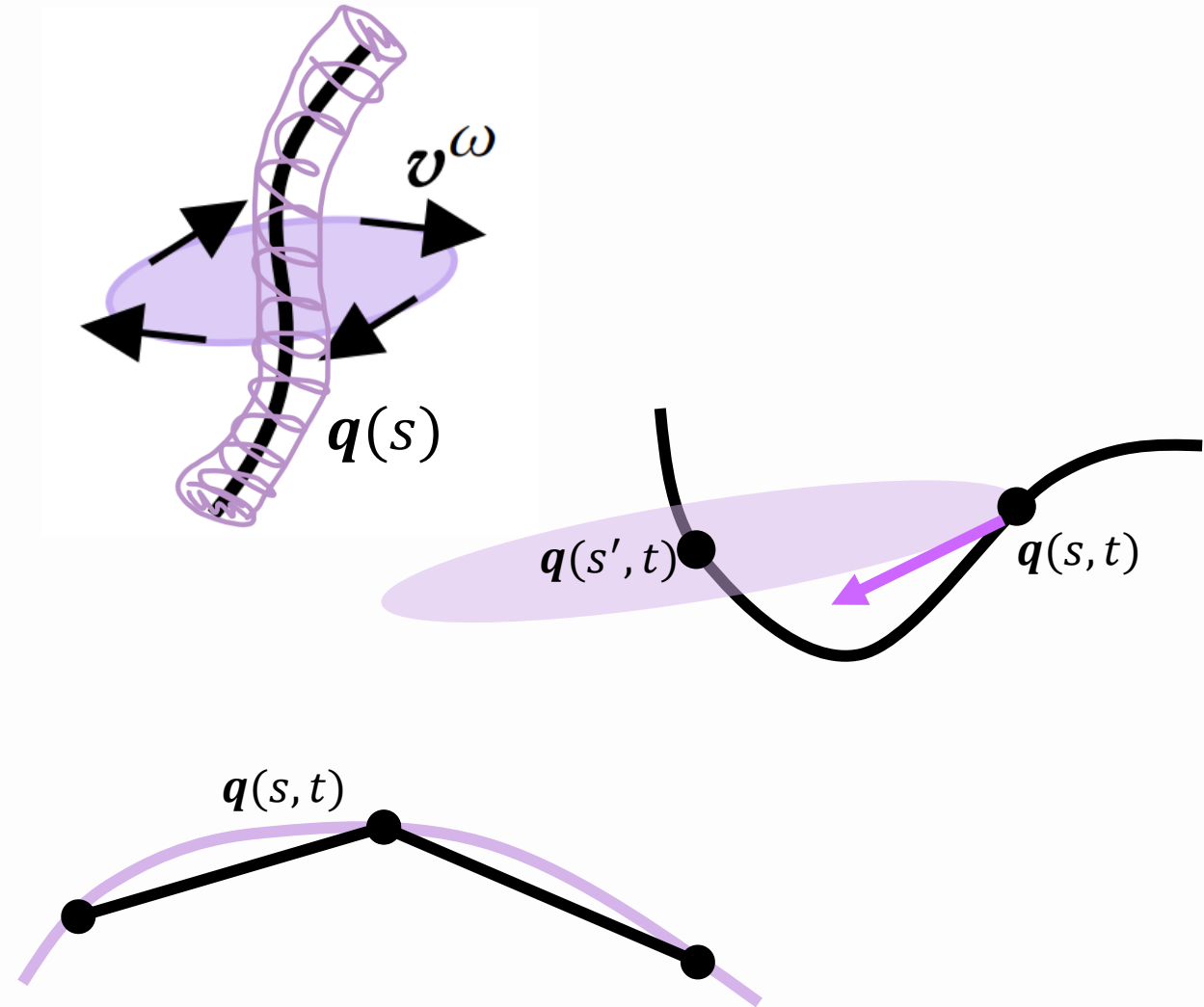
VORTEX FILAMENT KINEMATICS

- Velocity around a vortex filament, i.e., Biot-Savart law

$$\mathbf{v}^\omega(\mathbf{p}) = -\frac{\Gamma}{4\pi} \int_0^L \frac{(\mathbf{p} - \mathbf{q}(s)) \times \partial_s \mathbf{q}}{(\|\mathbf{p} - \mathbf{q}(s)\|^2 + \mu^2)^{\frac{3}{2}}} ds,$$

- Core kinematics by self-advection

$$\frac{\partial \mathbf{q}}{\partial t} = \mathbf{v}^\omega(\mathbf{q}) = -\frac{\Gamma}{4\pi} \int_0^L \frac{[\mathbf{q}(s, t) - \mathbf{q}(s', t)] \times \partial_{s'} \mathbf{q}}{(\|\mathbf{q}(s) - \mathbf{q}(s')\|^2 + \mu^2)^{\frac{3}{2}}} ds' = \mathbf{0}$$



VORTEX FILAMENT KINEMATICS

- Velocity around a vortex filament, i.e., Biot-Savart law

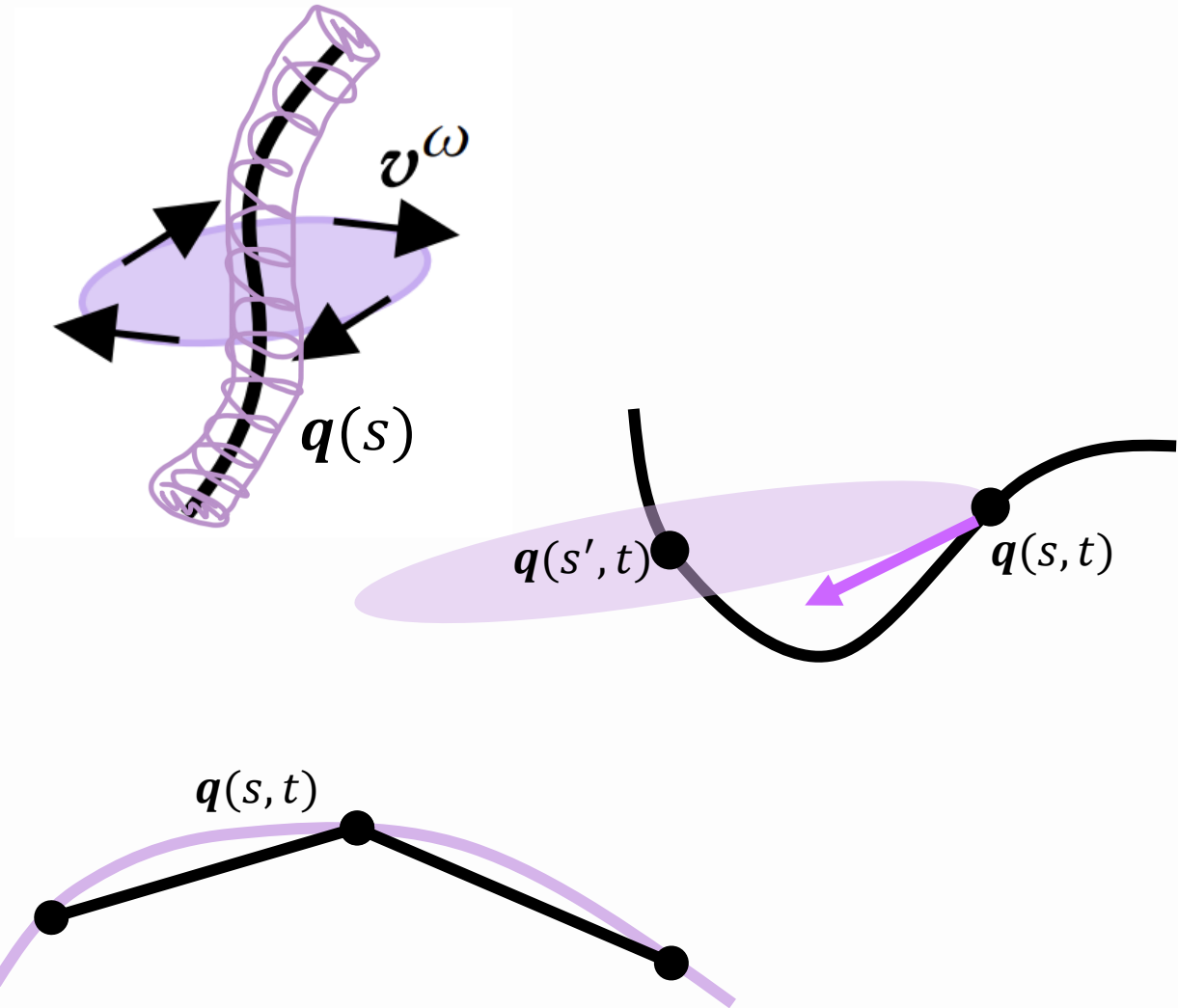
$$\mathbf{v}^\omega(\mathbf{p}) = -\frac{\Gamma}{4\pi} \int_0^L \frac{(\mathbf{p} - \mathbf{q}(s)) \times \partial_s \mathbf{q}}{(\|\mathbf{p} - \mathbf{q}(s)\|^2 + \mu^2)^{\frac{3}{2}}} ds,$$

- Core kinematics by self-advection

$$\frac{\partial \mathbf{q}}{\partial t} = \mathbf{v}^\omega(\mathbf{q}) = -\frac{\Gamma}{4\pi} \int_0^L \frac{[\mathbf{q}(s, t) - \mathbf{q}(s', t)] \times \partial_{s'} \mathbf{q}}{(\|\mathbf{q}(s) - \mathbf{q}(s')\|^2 + \mu^2)^{\frac{3}{2}}} ds' = \mathbf{0}$$

- Local induction approximation [Hama 1962]

$$\frac{\partial \mathbf{q}}{\partial t} = \mathbf{v}^{LIA}(\mathbf{q}) + \mathbf{v}^\omega(\mathbf{q}) = \frac{\Gamma}{4\pi} \left(\frac{\partial \mathbf{q}}{\partial s} \times \frac{\partial^2 \mathbf{q}}{\partial s^2} \right) \log \left(\frac{2\sqrt{l-l_+}}{e^{1/4} a} \right) - \frac{\Gamma}{4\pi} \int_0^L \frac{(\mathbf{q}(s) - \mathbf{q}(s')) \times \partial_{s'} \mathbf{q}}{(\|\mathbf{q}(s) - \mathbf{q}(s')\|^2 + \mu^2)^{\frac{3}{2}}} ds',$$



VORTEX FILAMENT KINEMATICS

- Velocity around a vortex filament, i.e., Biot-Savart law

$$\mathbf{v}^\omega(\mathbf{p}) = -\frac{\Gamma}{4\pi} \int_0^L \frac{(\mathbf{p} - \mathbf{q}(s)) \times \partial_s \mathbf{q}}{(\|\mathbf{p} - \mathbf{q}(s)\|^2 + \mu^2)^{\frac{3}{2}}} ds,$$

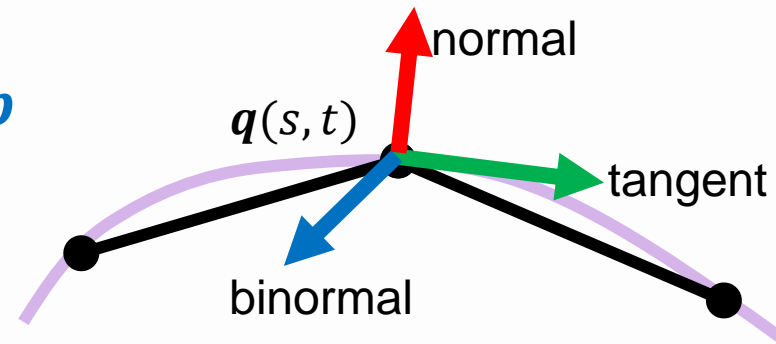
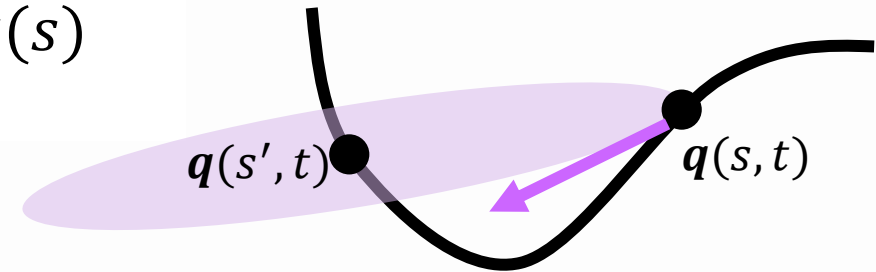
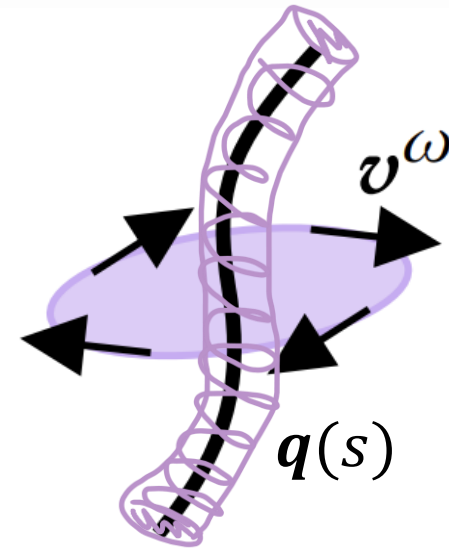
- Core kinematics by self-advection

$$\frac{\partial \mathbf{q}}{\partial t} = \mathbf{v}^\omega(\mathbf{q}) = -\frac{\Gamma}{4\pi} \int_0^L \frac{[\mathbf{q}(s, t) - \mathbf{q}(s', t)] \times \partial_{s'} \mathbf{q}}{(\|\mathbf{q}(s) - \mathbf{q}(s')\|^2 + \mu^2)^{\frac{3}{2}}} ds' = \mathbf{0}$$

- Local induction approximation [Hama 1962]

$$\frac{\partial \mathbf{q}}{\partial t} = \mathbf{v}^{LIA}(\mathbf{q}) + \mathbf{v}^\omega(\mathbf{q}) = \frac{\Gamma}{4\pi} \left(\frac{\partial \mathbf{q}}{\partial s} \times \frac{\partial^2 \mathbf{q}}{\partial s^2} \right) \log \left(\frac{2\sqrt{|l_- l_+|}}{e^{1/4} a} \right) \propto \kappa \mathbf{b}$$

$$- \frac{\Gamma}{4\pi} \int_0^L \frac{(\mathbf{q}(s) - \mathbf{q}(s')) \times \partial_{s'} \mathbf{q}}{(\|\mathbf{q}(s) - \mathbf{q}(s')\|^2 + \mu^2)^{\frac{3}{2}}} ds',$$



VORTEX FILAMENT KINEMATICS

- Velocity around a vortex filament, i.e., Biot-Savart law

$$\mathbf{v}^\omega(\mathbf{p}) = -\frac{\Gamma}{4\pi} \int_0^L \frac{(\mathbf{p} - \mathbf{q}(s)) \times \partial_s \mathbf{q}}{(\|\mathbf{p} - \mathbf{q}(s)\|^2 + \mu^2)^{\frac{3}{2}}} ds,$$

- Core kinematics by self-advection

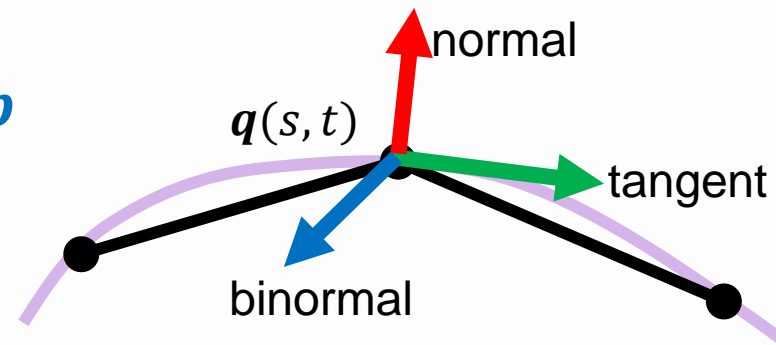
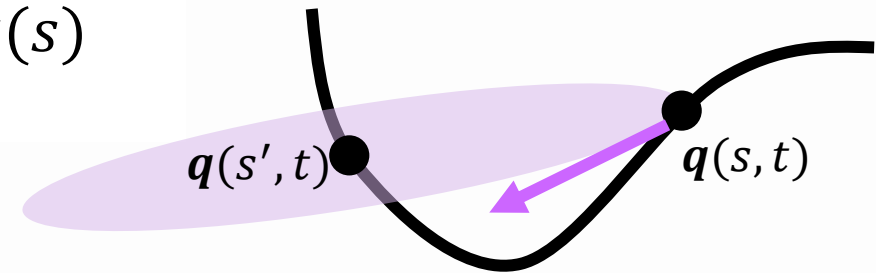
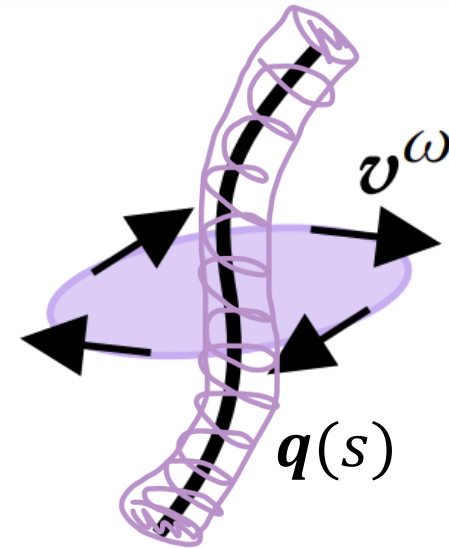
$$\frac{\partial \mathbf{q}}{\partial t} = \mathbf{v}^\omega(\mathbf{q}) = -\frac{\Gamma}{4\pi} \int_0^L \frac{[\mathbf{q}(s, t) - \mathbf{q}(s', t)] \times \partial_{s'} \mathbf{q}}{(\|\mathbf{q}(s) - \mathbf{q}(s')\|^2 + \mu^2)^{\frac{3}{2}}} ds' = \mathbf{0}$$

- Local induction approximation [Hama 1962]

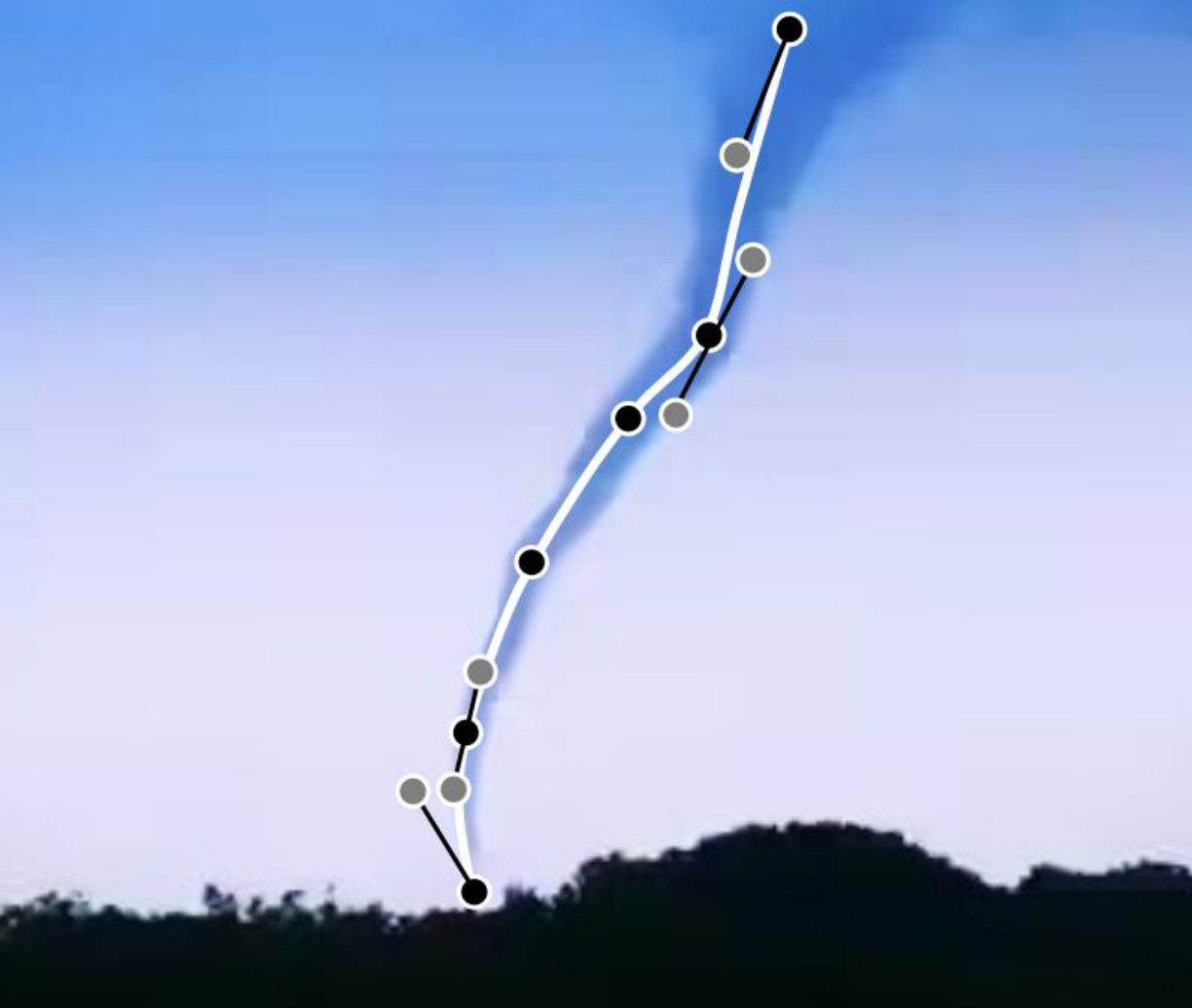
$$\frac{\partial \mathbf{q}}{\partial t} = \mathbf{v}^{LIA}(\mathbf{q}) + \mathbf{v}^\omega(\mathbf{q}) + \mathbf{v}^{env} \times \frac{\partial^2 \mathbf{q}}{\partial s^2} \log \left(\frac{2\sqrt{l-l_+}}{e^{1/4} a} \right) \propto \kappa \mathbf{b}$$

$$- \frac{\Gamma}{4\pi} \int_0^L \frac{(\mathbf{q}(s) - \mathbf{q}(s')) \times \partial_{s'} \mathbf{q}}{(\|\mathbf{q}(s) - \mathbf{q}(s')\|^2 + \mu^2)^{\frac{3}{2}}} ds',$$

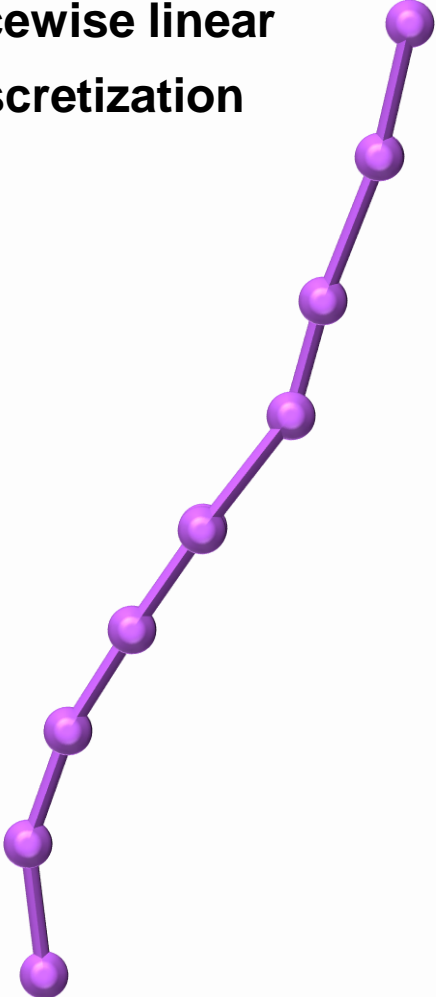
- Global environment velocity



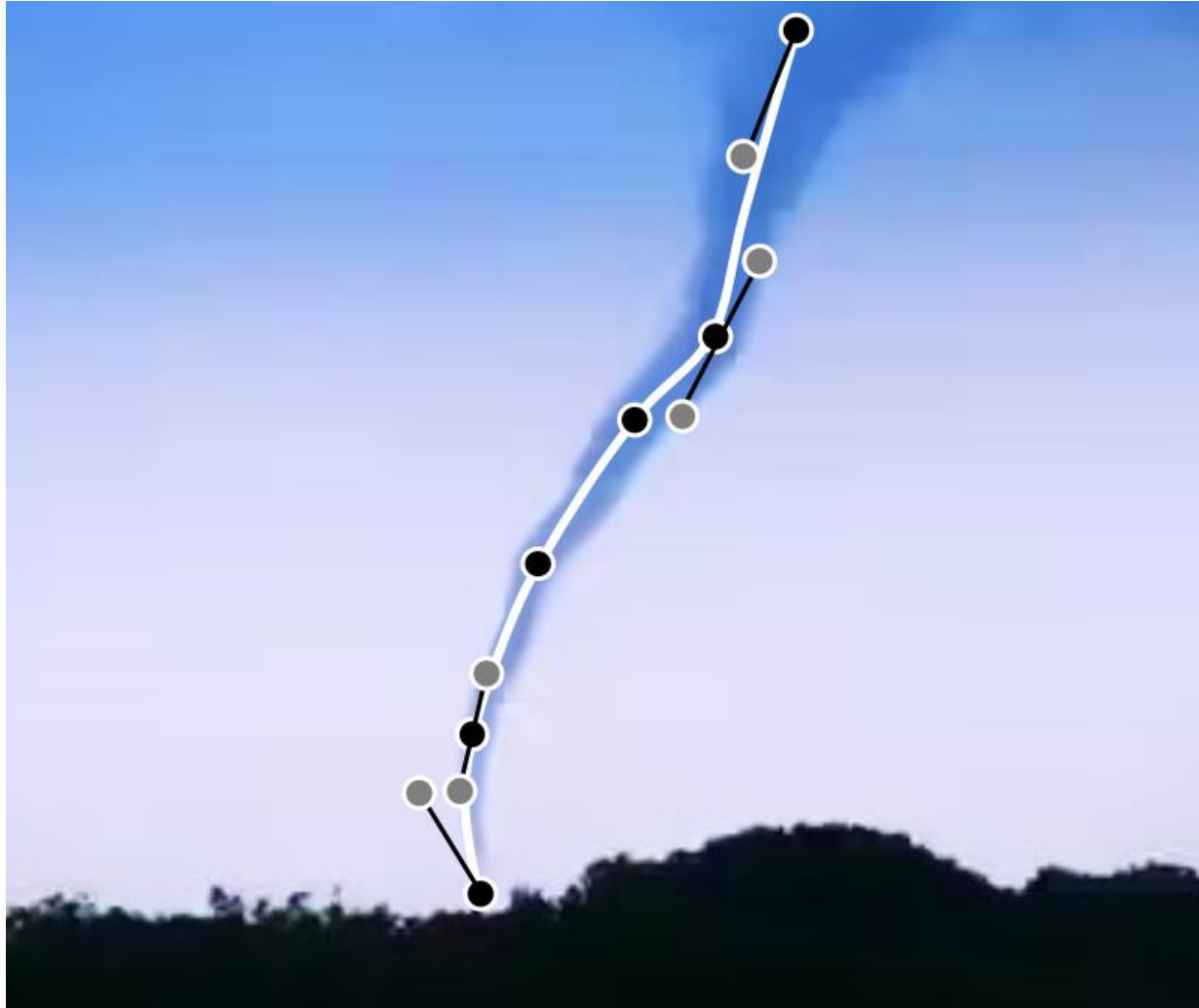
INITIALIZATION AND DISCRETIZATION



Piecewise linear discretization



INITIALIZATION AND DISCRETIZATION



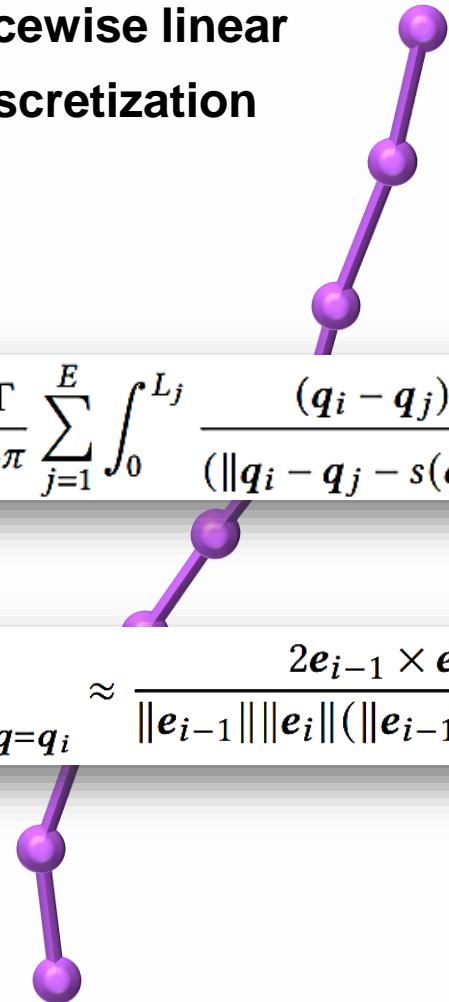
Piecewise linear
discretization

Velocity

$$v^\omega(q_i) = -\frac{\Gamma}{4\pi} \sum_{j=1}^E \int_0^{L_j} \frac{(q_i - q_j) \times (q_{j+1} - q_j)/L_j}{(\|q_i - q_j - s(q_{j+1} - q_j)/L_j\|^2 + \mu^2)^{\frac{3}{2}}} ds,$$

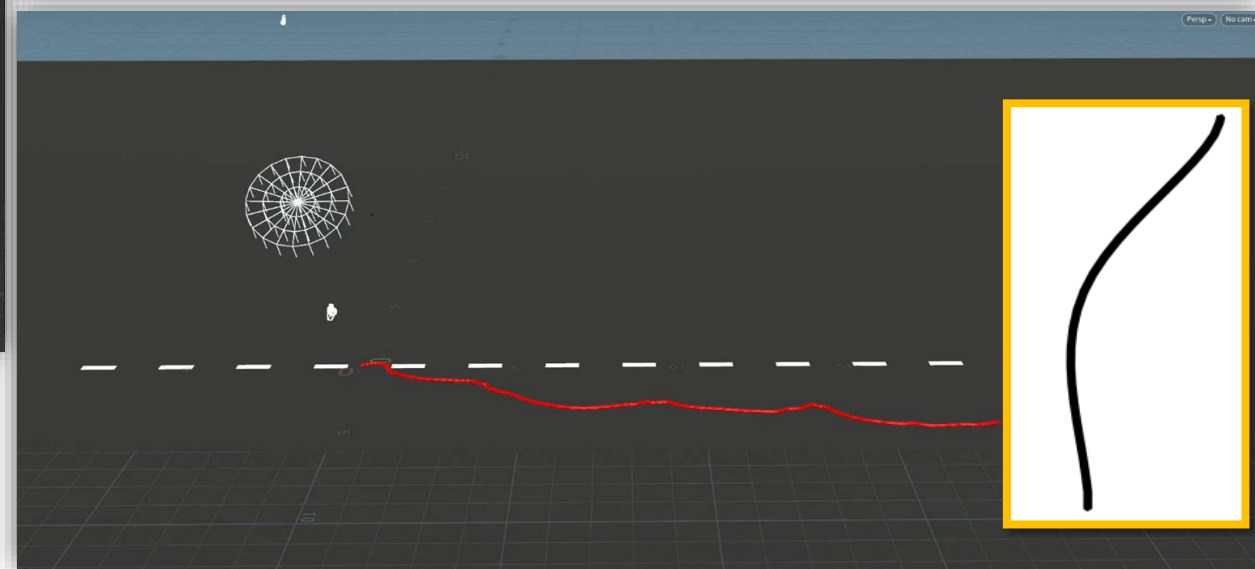
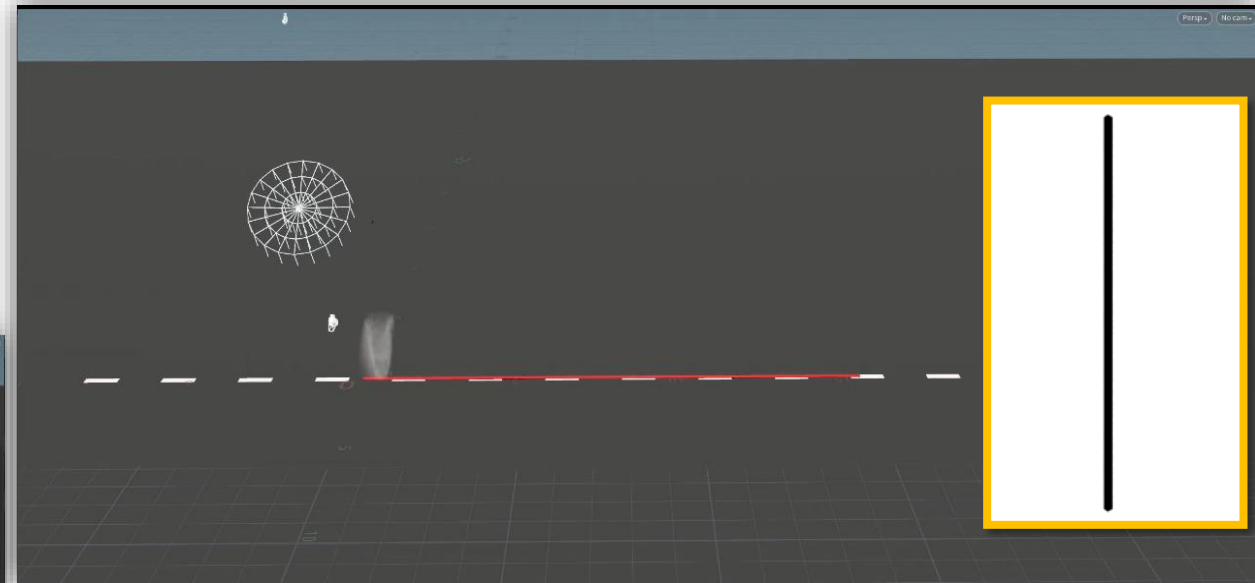
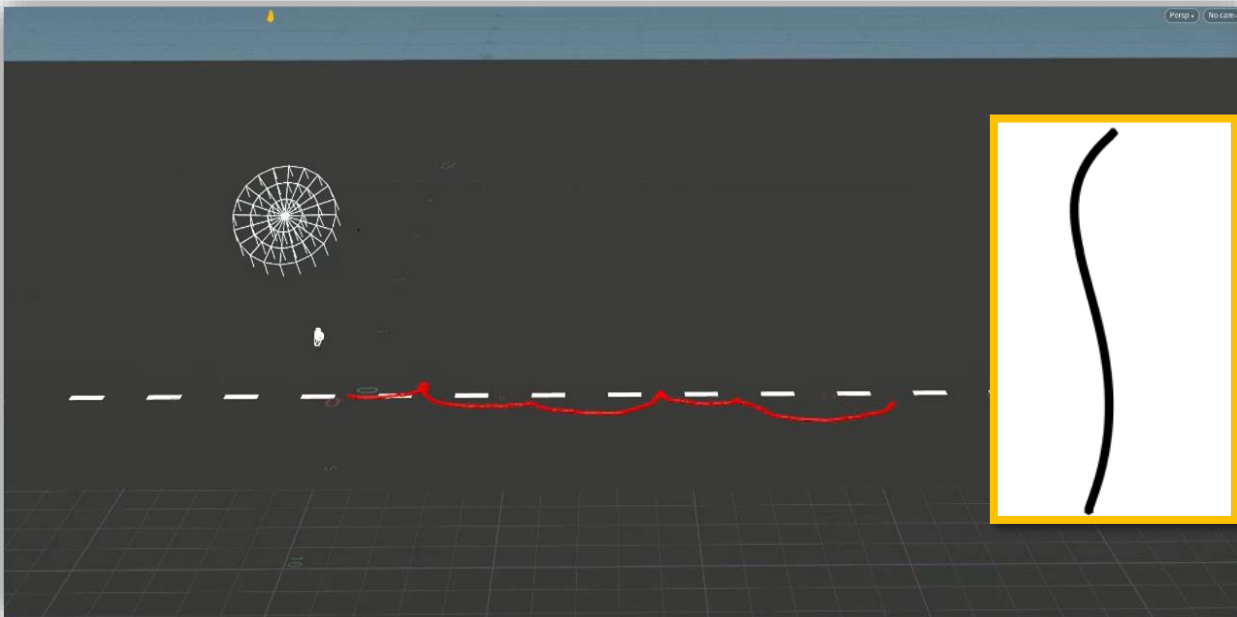
LIA

$$\left. \frac{\partial q}{\partial s} \times \frac{\partial^2 q}{\partial s^2} \right|_{q=q_i} \approx \frac{2e_{i-1} \times e_i}{\|e_{i-1}\| \|e_i\| (\|e_{i-1}\| + \|e_i\|)}, \quad e_i = q_{i+1} - q_i.$$



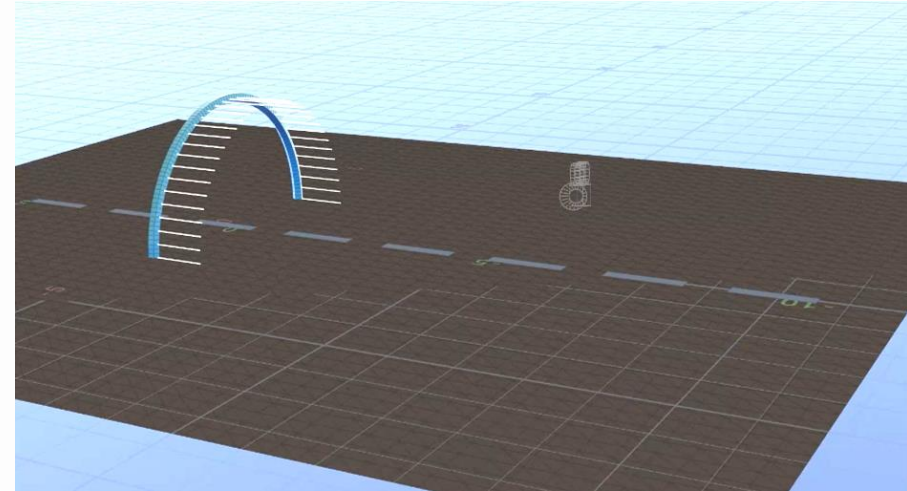
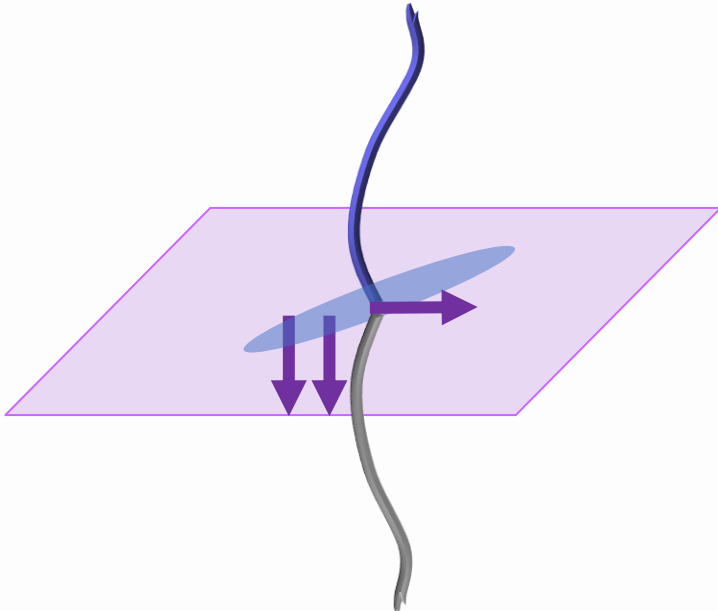
KINEMATICS FROM DIFFERENT INITIALIZATION

Curvature decides everything!



BOUNDARY CONDITION

- Boundary layer effect
 - Friction forces (viscosity, surface roughness) and centrifugal forces
 - High resolution discretization
- Non-penetration condition $\mathbf{n}^t \dot{\mathbf{q}}(s)|_{s=0} = 0$
 - For fundamental mass conservation law
 - Mirroring the filament [Schwarz 1985]

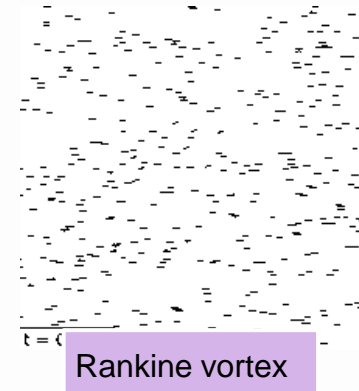
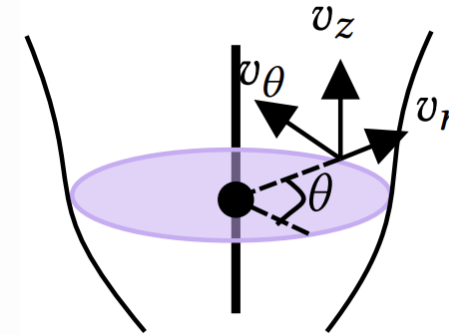


Water condensation funnel



AXISYMMETRIC FLOW

- Describe axisymmetric in cylindrical coordinates
 - Augment swirl flow (v_θ) with **radial** (v_r) and **axial** flow (v_z)
- Analytical vortex solution derived from the NS equations



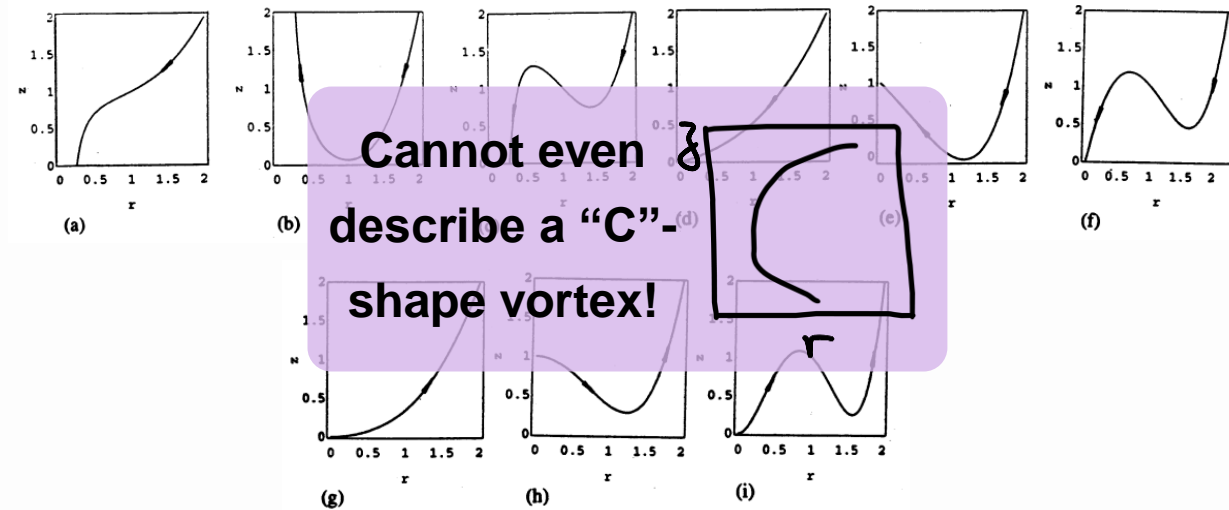
- Rankine vortex $v_r = 0, v_\theta(r) = \frac{\Gamma}{2\pi} \begin{cases} r/a^2 & r \leq a, \\ 1/r & r > a, \end{cases} v_z = 0$
- Burgers vortex $v_r = -\alpha r, v_z = 2\alpha z, v_\theta = \frac{\Gamma}{2\pi r} g(r)$
- Shtern's solution [Shtern et al. 1997]

$$\begin{cases} v_r = \mu Re/r, \\ v_\theta = \mu\Gamma/r, \\ v_z = \mu \left[W_c + W_p r^2 + W_r r^{Re} \right]. \end{cases}$$

Re : Reynolds number
 Γ : Circulation
 μ : Kinematic viscosity
 W_c, W_p, W_r : shear constants

- Funnel shape: zero level set of the **Stokes stream function**

$$\Psi(r, z) = \frac{W_c \mu}{2} r^2 + \frac{W_p \mu}{4} r^4 + \frac{W_r \mu}{2 + Re} r^{Re+2} - Re \mu z = 0.$$

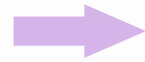


SPLINE-BASED VORTEX SOLUTION

- Let user design the Stokes stream function!

Radial and axial velocity

$$\begin{cases} v_r = -\frac{1}{r} \frac{\partial \Psi}{\partial z}, \\ v_z = +\frac{1}{r} \frac{\partial \Psi}{\partial r}. \end{cases}$$

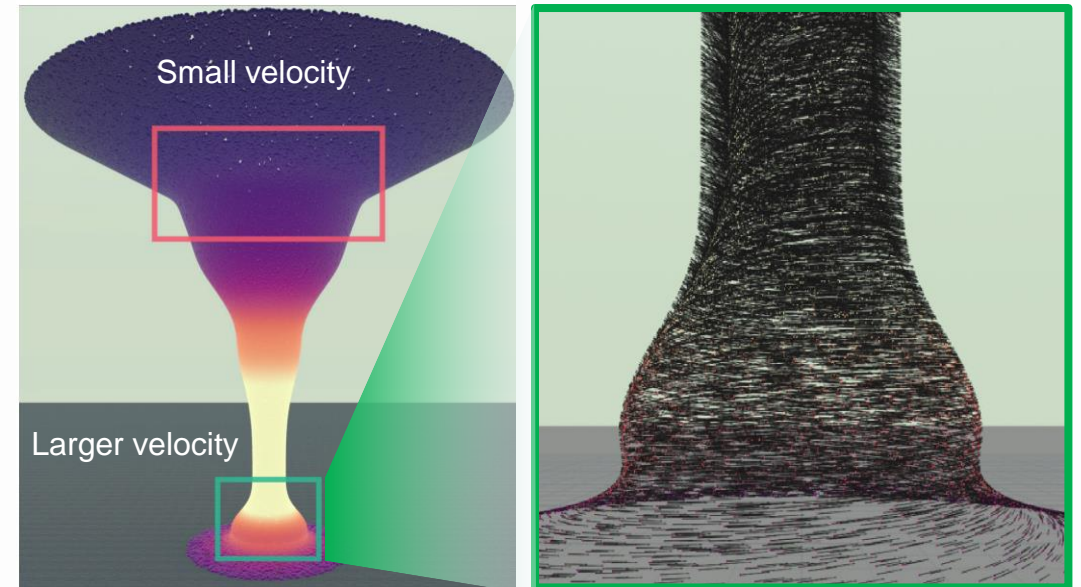
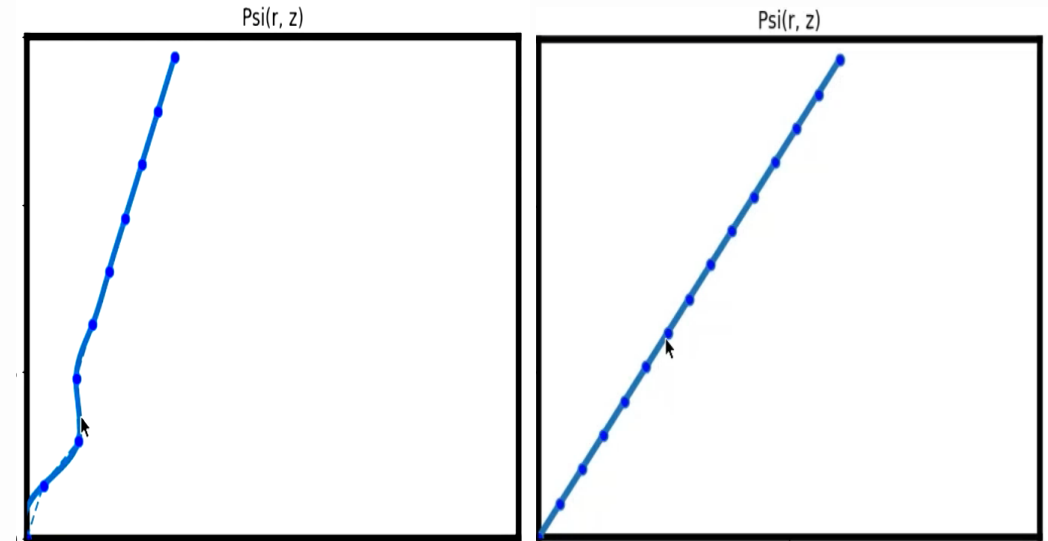


Continuity equation

$$\frac{1}{r} \frac{\partial(rv_r)}{\partial r} + \frac{\partial v_z}{\partial z} = 0,$$

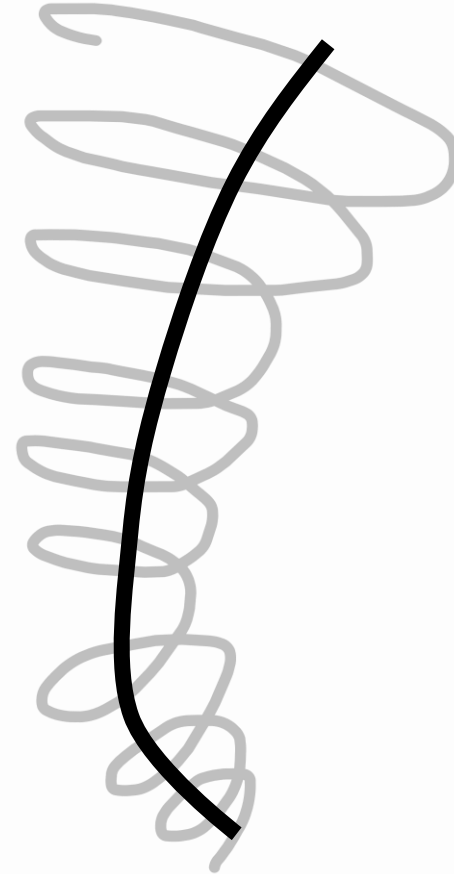
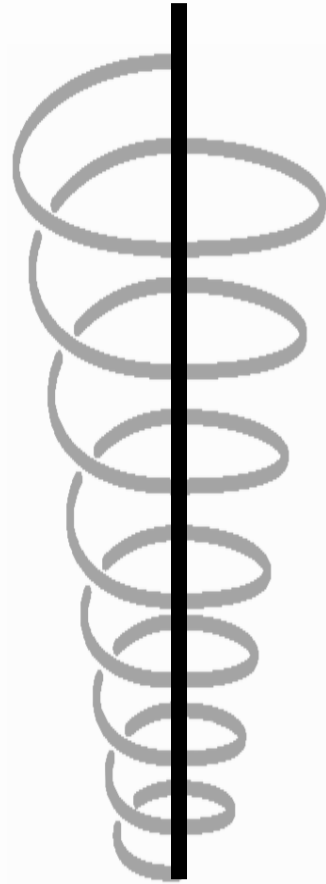
- No swirl velocity v_θ
- Couple with swirl velocity induced by the core

$$\begin{cases} v_r = \frac{\alpha}{r} \nabla_z f, \\ v_\theta = \frac{\Gamma}{2\pi r}, \\ v_z = \frac{\alpha}{r}. \end{cases}$$



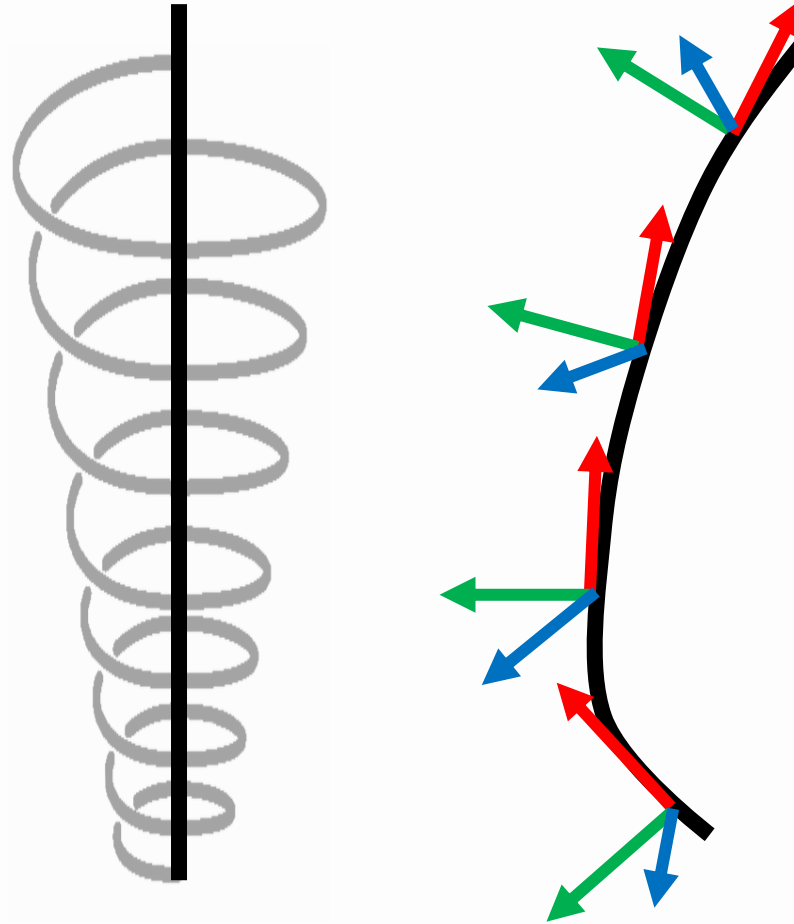
ADAPTING VORTEX TO A CURVED CORE

- From a rectilinear core to a curved one



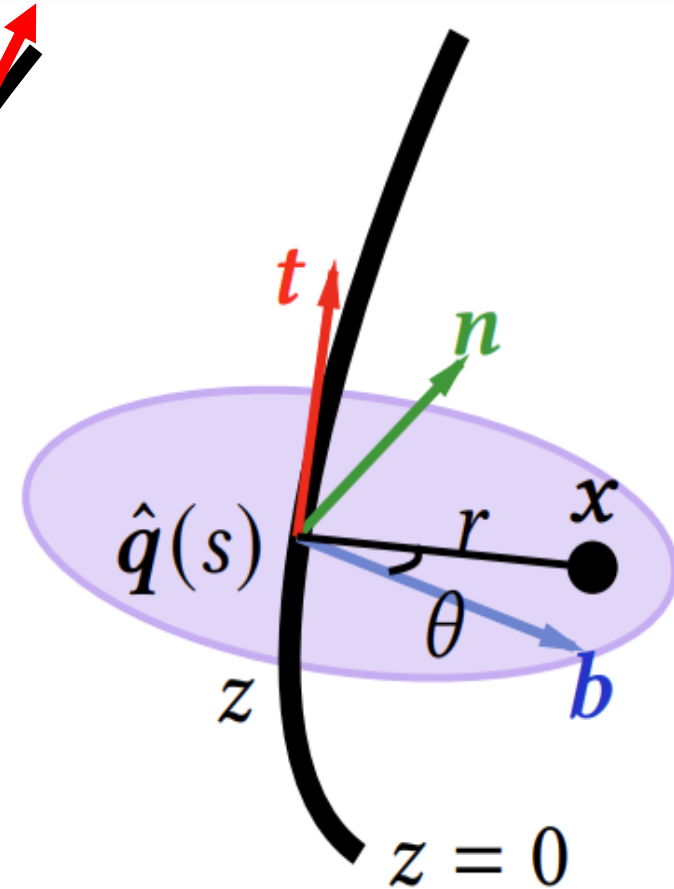
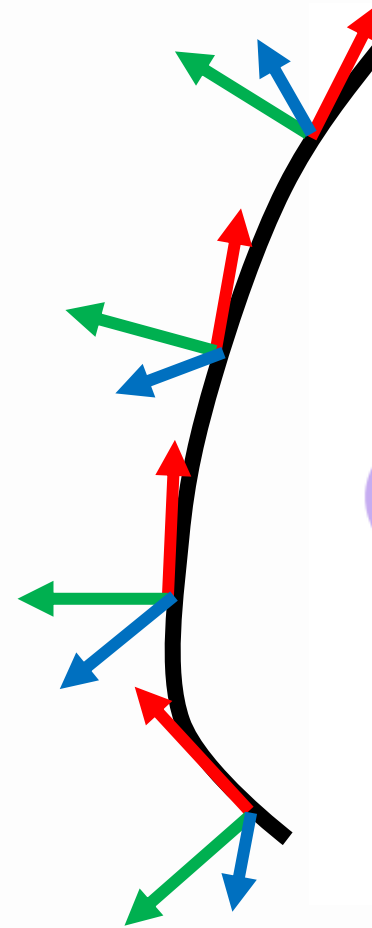
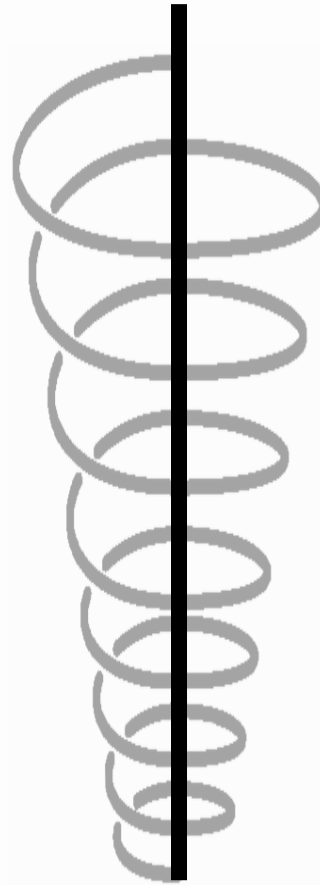
ADAPTING VORTEX TO A CURVED CORE

- From a rectilinear core to a curved one
 - Update the material frame



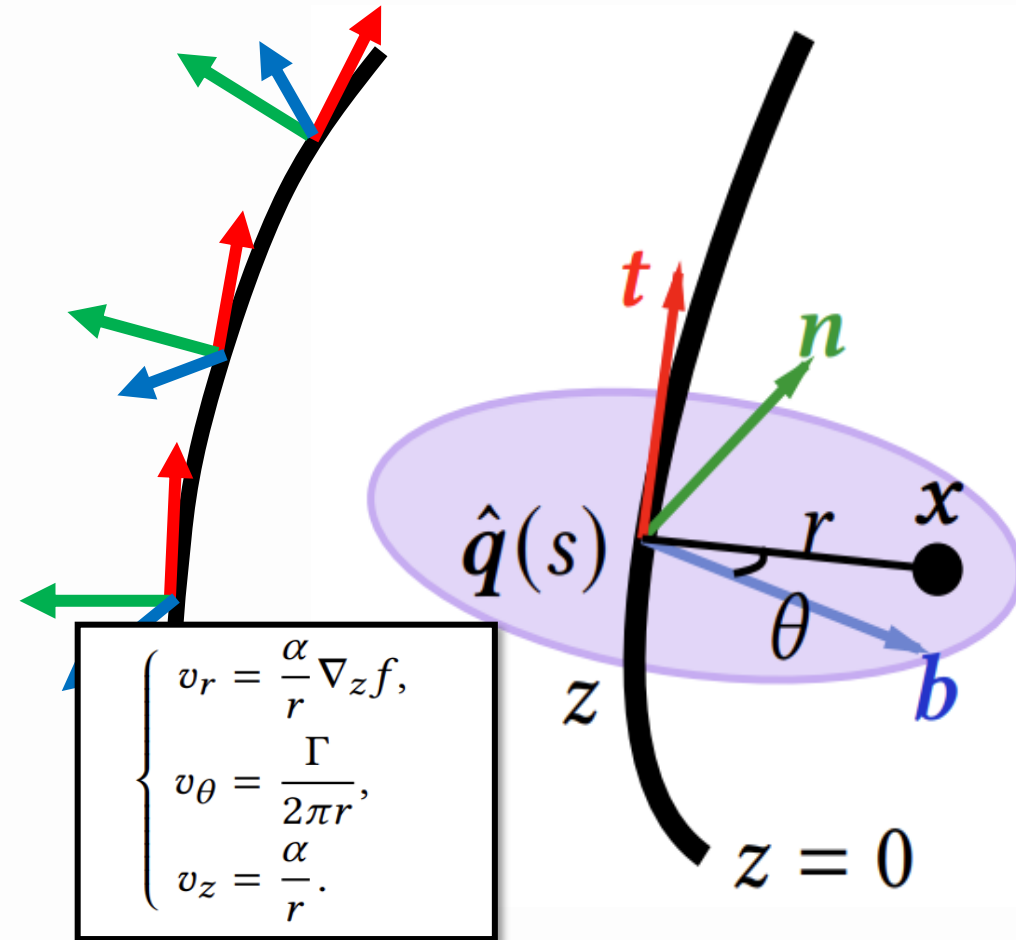
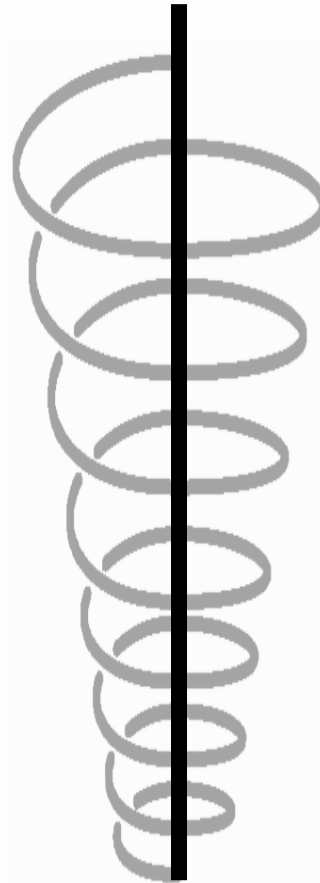
ADAPTING VORTEX TO A CURVED CORE

- From a rectilinear core to a curved one
 - Update the material frame
 - Compute local cylindrical coordinates at the given point



ADAPTING VORTEX TO A CURVED CORE

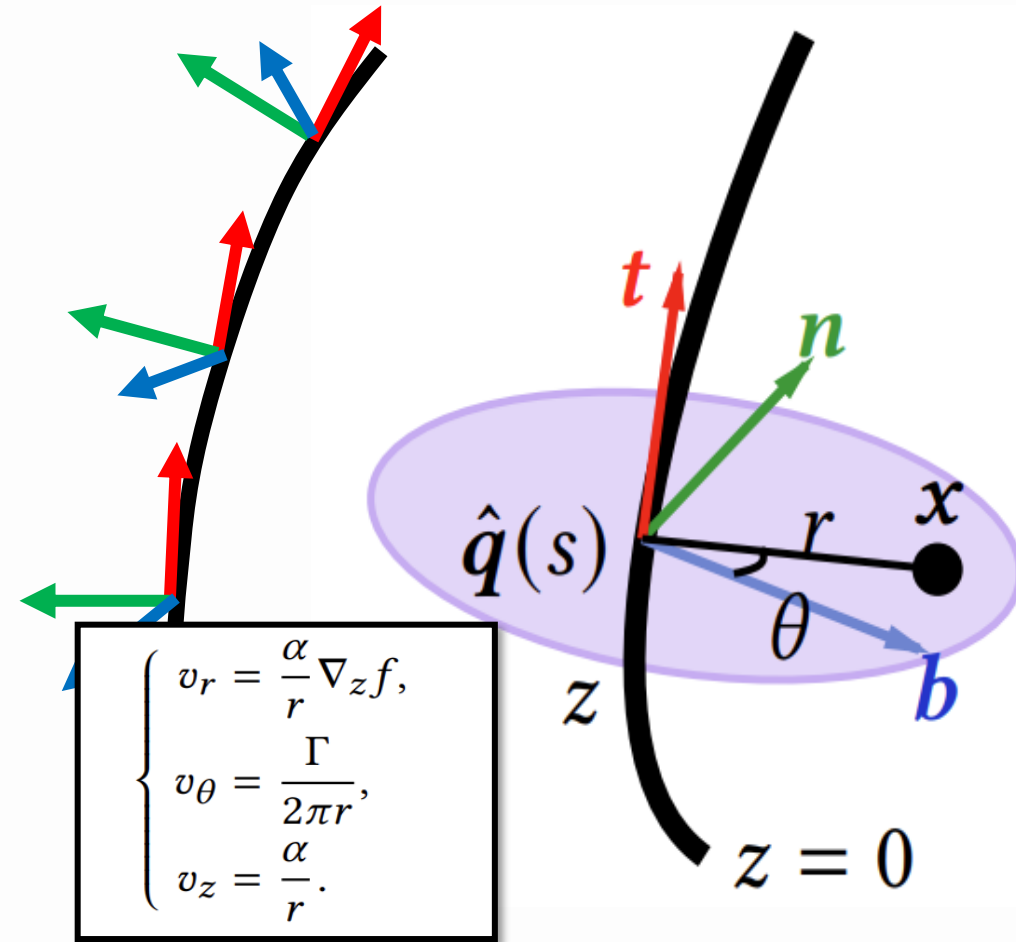
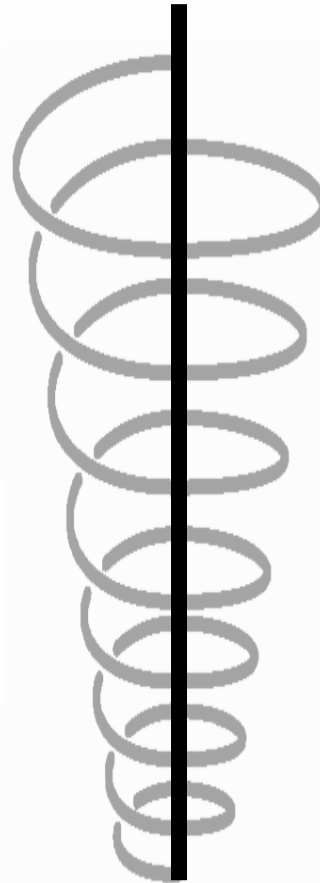
- From a rectilinear core to a curved one
 - Update the material frame
 - Compute local cylindrical coordinates at the given point
 - Compute the vortex velocity in the local frame



ADAPTING VORTEX TO A CURVED CORE

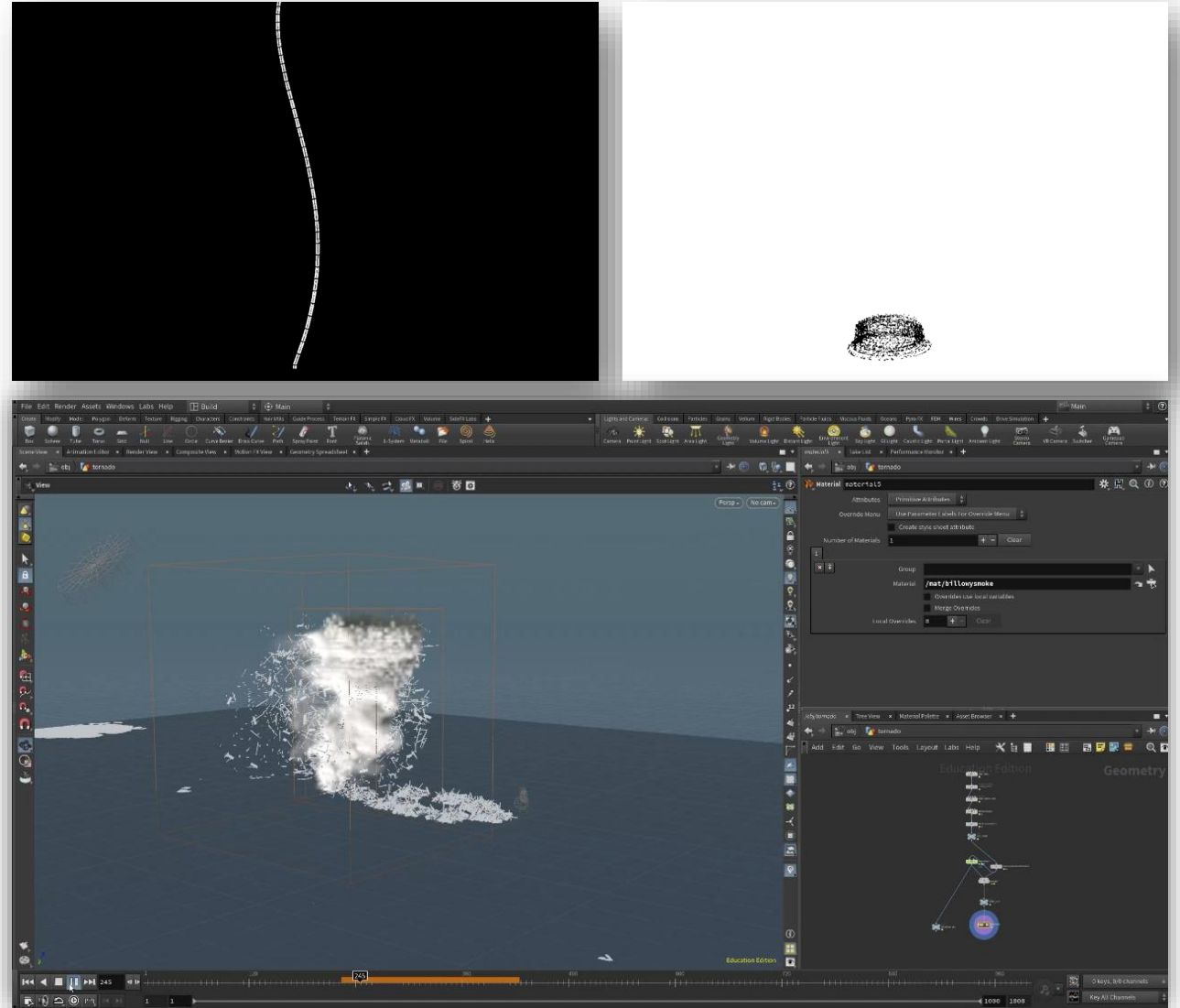
- From a rectilinear core to a curved one
 - Update the material frame
 - Compute local cylindrical coordinates at the given point
 - Compute the vortex velocity in the local frame
 - Transform the local velocity to the global frame

$$\mathbf{v}(\mathbf{x}) = (\mathbf{b}(s) \ \mathbf{n}(s) \ \mathbf{t}(s)) \begin{pmatrix} \cos(\theta)v_r - \sin(\theta)v_\theta \\ \sin(\theta)v_r + \cos(\theta)v_\theta \\ v_z \end{pmatrix}.$$

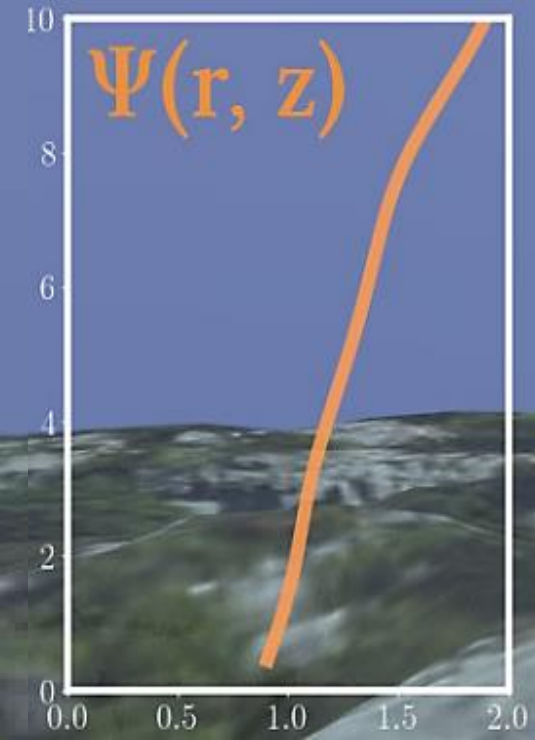


IMPLEMENTATION

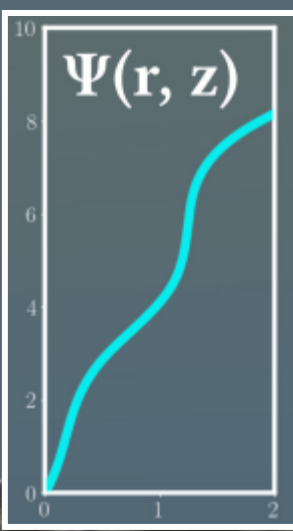
- Numerical integration (C++)
 - Compute the kinematics of the core
 - Randomly sample particles around the core, and advect them in the vortex velocity field
 - Less than 30ms per step for 15k particles
- Procedural refinement (Houdini)
 - Import the particles and their attributes
 - Add turbulence
 - Transport rigid bodies
 - Volume rendering
- Example code
 - <https://gitlab.inria.fr/geomerix/public/twisterforge>



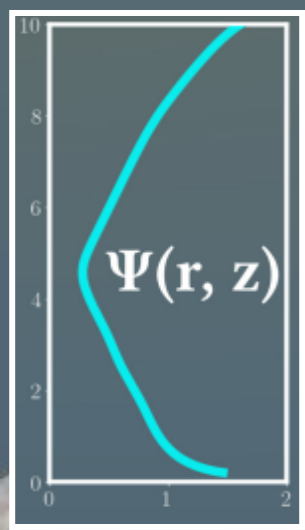
NON-EVEN TERRAIN



CONTROL OVER THE FUNNEL PROFILE

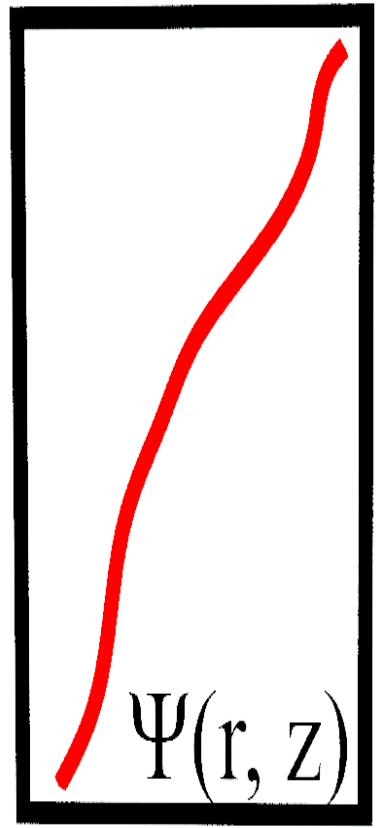
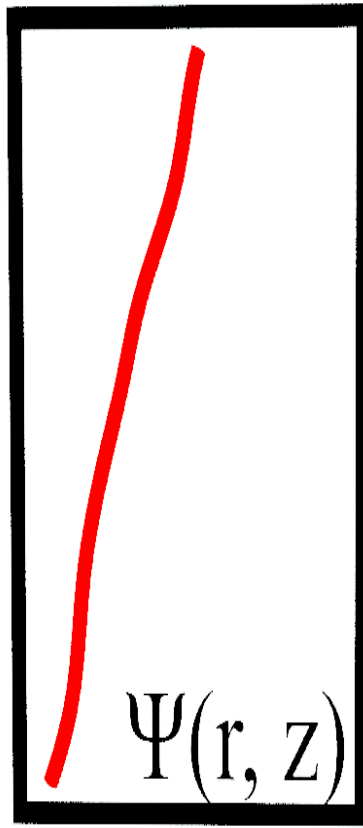
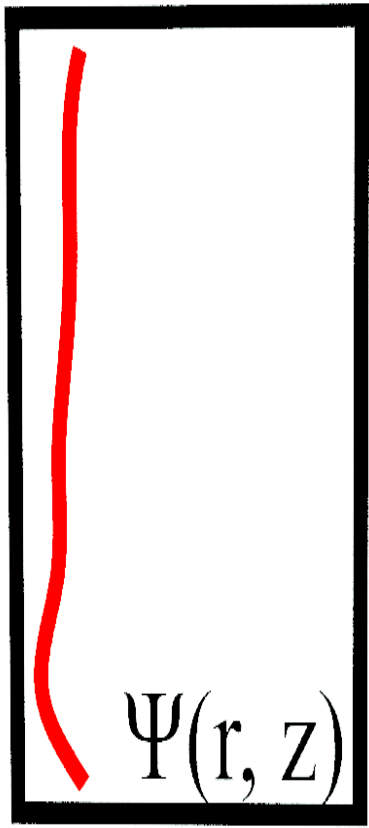


CONTROL OVER THE FUNNEL PROFILE



FROM STEADY TO NON-STEADY FLOW

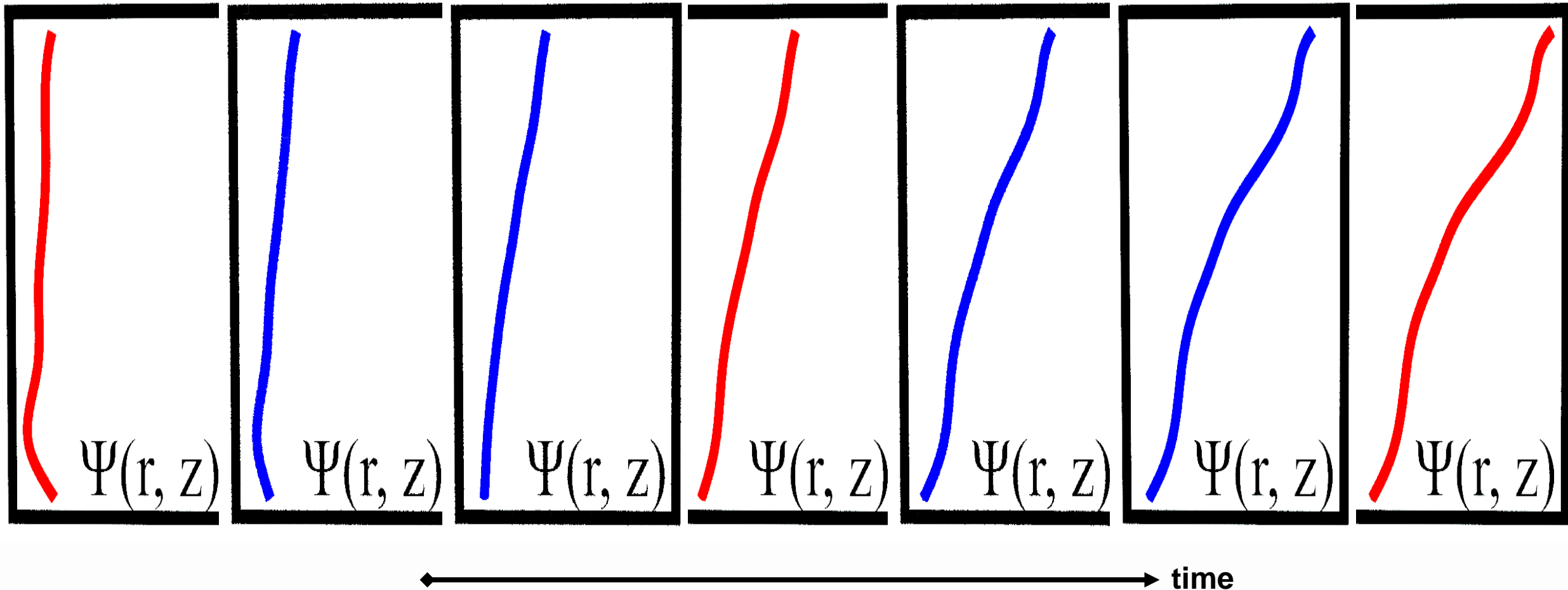
- Spline parameterization allows for easy interpolation in time



← time →

FROM STEADY TO NON-STEADY FLOW

- Spline parameterization allows for easy interpolation in time




INTERPOLATING THE PROFILE

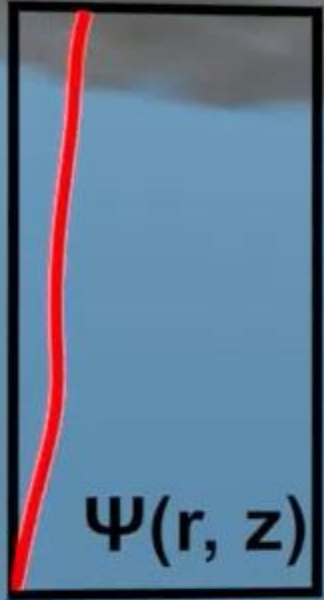
replay with keyframes frozen

keyframe



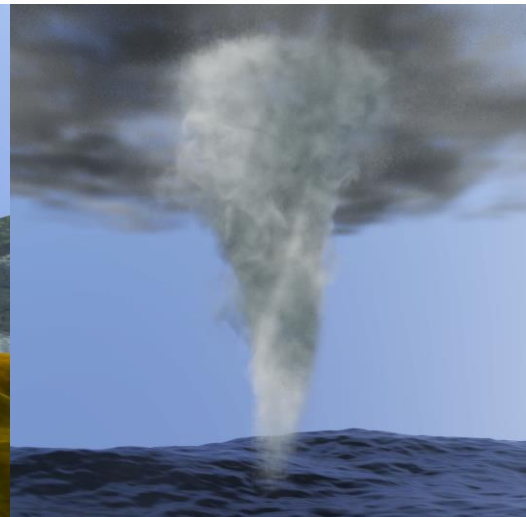
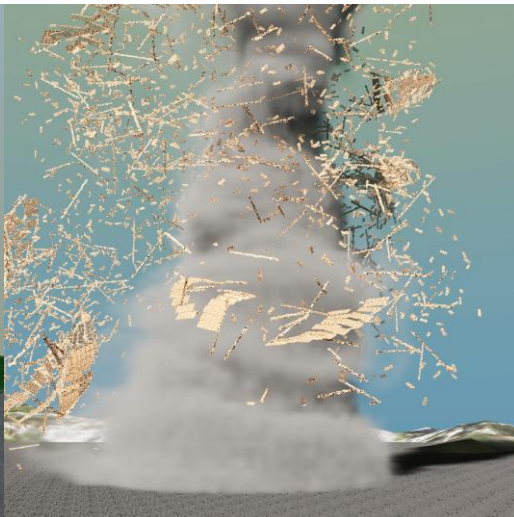
IMITATING THE LIFE CYCLE

 replay with keyframes frozen



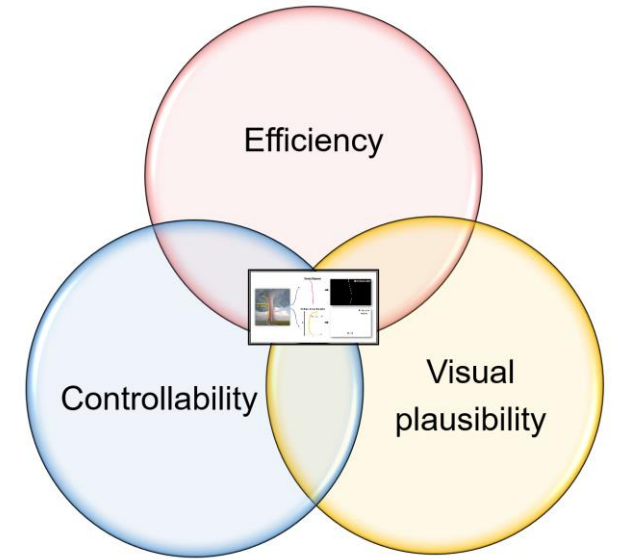
keyframe

VIRTUAL VS. REAL



CONCLUSION

- Contribution
 - A flexible authoring tool for **controllable**, **efficient** and **plausible** tornado animations
- Limitations
 - Our vortex model is not physically accurate
 - The spline-derived vortex violates the NS equation in general
 - Temporal interpolation can be far from the real dynamics
 - The core and the funnel are loosely coupled
 - Boundary conditions are oversimplified
 - More to consider, such as viscosity, friction, surface roughness
 - Interaction with solid bodies
 - Two-way coupling, i.e., solids should affect the tornado dynamics as well



A scenic view of a city skyline reflected in a lake, with cherry blossom trees in the foreground. The sky is clear and blue, and the water is calm, reflecting the buildings and trees. The cherry blossom trees are in full bloom, with light purple flowers. The city skyline includes several tall buildings, some with unique architectural features like a pyramid-shaped top.

Thanks!

MIG
2024
Arlington